HOMOZYGOUS DELETIONS LOCALIZE NOVEL TUMOR SUPPRESSOR GENES IN B-CELL LYMPHOMAS

Cinta Mestre-Escorihuela[1], Fanny Rubio-Moscardo[1], Jose A Richter[1], Reiner Siebert[2], Joan Climent[1], Vicente Fresquet[1], Elena Beltran[1], Xabier Agirre[1], Isabel Marugan,[3] Miguel Marín[3], Andreas Rosenwald[4], Kei-ji Sugimoto[5], Luise M. Wheat[5], E. Loraine Karran[5], Juan F. García,[6] Lydia Sanchez,[6] Felipe Prosper[1], Louis M. Staudt[7], Daniel Pinkel[8], Martin J.S. Dyer[5], Jose A. Martinez-Climent[1]

AFFILIATIONS: (1) Center for Applied Medical Research (CIMA), Division of Oncology, University of Navarra, Pamplona, Spain; (2) Institute of Human Genetics, University Hospital Schleswig-Holstein, Kiel, Germany; (3) Department of Hematology and Medical Oncology, Hospital Clínico, University of Valencia, Spain; (4) Department of Pathology, University of Würzburg, Germany (5) MRC Toxicology Unit, University of Leicester, UK; (6) Molecular Pathology Program, National Center for Oncology Research (CNIO, Madrid, Spain); (7) National Cancer Institute, NIH, Bethesda, MD, USA; and (8) Cancer Research Institute, University of California San Francisco, CA, USA

SHORT TITLE: Novel tumor suppressors in lymphoma

CORRESPONDING AUTHOR: Jose A. Martinez-Climent, M.D., Ph.D., Division of Oncology, Center for Applied Medical Research (CIMA). University of Navarra. Avda Pio XII, 55. Pamplona 31008 (SPAIN). Tel: 34-948-194700-ext 1029; Fax: 34-948-194714; e-mail: jamcliment@unav.es

MANUSCRIPT INFORMATION: 1 Table; 6 color Figures; Supplemental material (3 Web Tables and 3 Web Figures)

WORD AND CHARACTER COUNTS: 200 words in abstract; 4.998 characters in the paper.

GRANT SUPPORT: This work was supported by grants from the Spanish Ministry of Education and Science (SAF-5340/2005 and Ramon-Cajal Programme), International Union Against Cancer (UICC-YY1/05/006), Spanish Hematology Association (AEHH), Navarra Government (Education Council), European Commission (VI Framework Programme LSHC-CT-2004-503351), Deutsche Krebshilfe, Lymphoma Research Foundation (NY), Medical Research Council and UTE-FIMA

AUTHOR´S CONTRIBUTION: Cinta Mestre performed research, analyzed data and designed research; Fanny Rubio-Moscardo, Jose Richter, Joan Climent, Reiner Siebert, Andreas Rosenwald, Kei-ji Sugimoto, Luise M. Wheat, E. Loraine Karran, Miguel Marín and Juan F. García performed research and analyzed data; Isabel Marugan, Louis M. Staudt and Daniel Pinkel contributed new reagents or analytical tools; Martin J.S. Dyer designed research and analyzed data; Jose A. Martinez-Climent designed research, performed research, analyzed data and wrote the paper.

ABSTRACT

Integrative genomic and gene expression analyses have identified amplified oncogenes in B-cell non-Hodgkin lymphoma (B-NHL), but the capability of such technologies to localize tumor suppressor genes within homozygous deletions remains unexplored. Array-based comparative genomic hybridization (CGH) and gene expression microarray analysis of 48 cell lines derived from patients with different B-NHLs delineated twenty homozygous deletions at seven chromosome areas, all of which contained tumor suppressor gene targets. Further investigation revealed that only a fraction of primary biopsies presented inactivation of these genes by point mutation or intragenic deletion, but instead some of them were frequently silenced by epigenetic mechanisms. Notably, the pattern of genetic and epigenetic inactivation differed among B-NHL subtypes. Thus, the P53-inducible *PIG7/LITAF* was silenced by homozygous deletion in primary mediastinal B-cell lymphoma and by promoter hypermethylation in germinal center lymphoma, the pro-apoptotic *BIM* gene presented homozygous deletion in mantle cell lymphoma and promoter hypermethylation in Burkitt lymphoma, pro-apoptotic BH3-only NOXA was mutated and preferentially silenced in diffuse large B cell lymphoma and *INK4c/P18* was silenced by bi-allelic mutation in mantle cell lymphoma with unmutated *IGH* gene. Our microarray strategy has identified novel candidate suppressors inactivated by genetic and epigenetic mechanisms that substantially vary among the B-NHL subtypes.

INTRODUCTION

The B-cell non-Hodgkin lymphomas (B-NHLs) comprise various distinct clinico-pathological entities that in most instances are characterized by recurrent chromosomal translocations involving the immunoglobulin (*IG*) gene loci.[1] *IG* chromosomal translocations are thought to be early events in the pathogenesis of these malignancies and result in deregulated expression of a variety of oncogenes involved in cell proliferation, differentiation pathways and apoptosis regulation. However, they are not usually sufficient for tumor formation and the accumulation of other genetic aberrations is critical for the acquisition of the full neoplastic phenotype.[2] Comparative genomic hybridization (CGH) and CGH to BAC microarray techniques have identified recurrent regions of amplification and deletion, many of which are predicted to encode oncogenes and tumor suppressor genes that are important for tumorigenesis.[3-9] The impact of DNA amplification on gene expression variation has been investigated at the genome scale in breast cancer,[10] lung cancer,[11] pancreatic adenocarcinoma,[12] and B-cell lymphoma.[13,14] These and other reports led to the positional identification of over-expressed genes mapped at the peaks of amplification in tumor cells.[4,13,15-18] However, the capability of array-based CGH combined with gene expression microarrays to carry out genome-wide screens for regions of deletion that may harbor putative tumor suppressor genes in B-NHL has not been explored yet.

To discover tumor suppressor genes with previously unknown relevance in lymphoma that may be silenced by homozygous deletion, we applied high-resolution BAC array CGH and gene expression profiling microarrays to a panel of 48 cell lines derived from patients with the different B-NHL subtypes.[19,20] We identified twenty homozygous deletions at seven different chromosome areas. Delineation of these loci and search for contained genes with reduced expression revealed known suppressor genes as well as novel putative targets that were further characterized in cell

lines and in primary lymphoma biopsies by FISH analysis, mutation screening and promoter methylation studies, quantitative real-time PCR, Western blot and immunohistochemistry on tissue microarrays. Our data demonstrate that array CGH combined with gene expression profiling provide a rationale for discovering tumor suppressor genes in regions of homozygous loss. These target genes show different patterns of gene inactivation that vary among the B-NHL subtypes.

MATERIAL AND METHODS

TUMOR CELL LINES: A panel of forty-eight cell lines derived from patients comprising the various subtypes of B-NHL was studied: Granta 519, HBL2, SP49, Z138, REC1, NCEB1, JVM2, UPN1, UPN2, SP53, JEKO1 and IRM2 (mantle cell lymphoma; n=12); OZ, VAL, Karpas 422, DOHH2, Karpas 353, PR1, OCI-LY8, Karpas 231, SUDHL6, ROS-50, RL, SCI1, BEVA, Granta 452 and 380 (diffuse large B cell lymphoma with the translocation t(14;18)(q32;q21); n=15); MD901, MD903, RIVA, CTB1, RCK8 and CIPULLO (diffuse large B-cell lymphoma lacking t(14;18)(q32;q21) translocation; n=6); ELIJAH, NAB2, PL29018, SERAPHINA, Wien-133, P32, BALM9, CA46, Namalwa, BL41 and KHM10B (Burkitt lymphoma; n=11), SSK41 and Karpas 1718 (marginal zone lymphoma); and Karpas 1106 and MEDB1 (primary mediastinal B-cell lymphoma).

CYTOGENETIC ANALYSES. Twenty-five of the cell lines (those underlined) were studied by G-banding cytogenetics and standard CGH to chromosomes (s-CGH). In fifteen of them showing complex karyotypes, additional color cytogenetic analysis including cross-species color banding (RxFISH, Cambio), spectral karyotyping (SKY, Applied Spectral Imaging), and/or multicolor FISH (SpectraVysion, Vysis),

FLUORESCENCE IN SITU HYBRIDIZATION (FISH). To classify the cell lines into clinical-pathological B-NHL subgroups according to the presence of chromosomal translocations and to confirm the DNA copy number changes obtained from array CGH studies, FISH analysis using individual probes was performed on fixed cells from selected cell lines. These BAC and PAC probes corresponded to *IGH, CCND1*, *BCL2*, *BCL6*, *MALT1, MYC* and *CDK6* gene loci. In addition, BACs RP11-233N20 (3q29), RP11-215F02 (11p13), RP11-89M8 (8p21.3) and RP11-165N12 (13q31.3) were also used. To further delineate the 16p13.13 genomic deletion, we also hybridized BACs RP11-89D3, RP11-109M19, RP11-66H6, RP11-396B14, RP11-547D14,

RP1149M6, RP11-394B14, and RP11-165B11 in cells from Karpas 1106 cell line. These clones were purchased from Research Genetics (Huntstville, AL, USA), Vysis (Downers Grove, IL, USA), or RZPD German Resource Center (Berlin, Germany).

MICROARRAY-BASED COMPARATIVE GENOMIC HYBRIDIZATION AND DATA ANALYSIS: Genome-wide analysis of DNA-copy number changes of the 48 cell lines was performed using array CGH on a microchip with ~2.400 BAC and P1 clones in triplicate. The array provides an average resolution of 1.4 Mb across the genome. Production and validation of the array, hybridization methods and analytical procedures have been described elsewhere.[5,19] For delineation of common regions of genomic imbalance in the lymphoma genomes, the position of the BAC/PACs on the draft human genome sequence according to the May 2004 freeze was used (http://genome.cse.ucsc.edu). For visualization of genomic data, the TreeView program 1.60 (Stanford, CA) was used. Microarray data has been deposited in GEO database (GPL37898).

GENE EXPRESSION MICROARRAY ANALYSIS: To investigate the level of expression of the genes mapped across the common regions of genomic gain and loss, the "Lymphochip" cDNA microarrays were used for the gene expression profiling of 32 of the B-NHL cell lines, as previously reported.[20] In 8 mantle cell lymphoma cell lines (Granta 519, HBL2, SP49, NCEB1, JVM2, UPN1, JEKO1 and IRM2), Affymetrix Gene Chips Human Genome U133 microarray studies were also performed according to the manufacturer´s instructions.

REAL-TIME QUANTITATIVE POLYMERASE CHAIN REACTION (QRT-PCR): To validate the data from the cDNA microarrays for *CDK6* and *NOXA*, the same RNA aliquots used in the cDNA microarray analysis were studied using QRT-PCR, as previously described.[17] To study the expression levels of *PIG7/LITAF* and *BIM*, QRT-PCR was performed in an ABI PRISM 7500 Sequence Detection System (Applied Biosystems, Weitersadt, Germany) using the Assay-on-Demand Gene Expression product for *PIG7/LITAF* (ABI-Hs.00191583) and *BIM* (ABI-

Hs.00197982). The mRNA expression was normalized by using *GAPDH* gene product as endogenous control of expression (ABI-Hs.99999905).

DELINEATION OF HOMOZYGOUS DELETIONS: To confirm homozygous deletion according to array CGH data, PCR on genomic DNA was performed in the corresponding cell lines. Additional primer sets were designed and applied to further narrow down the regions of deletion.

WESTERN BLOTTING OF CELL LINES AND PRIMARY B-NHL SAMPLES: A number of deregulated genes (CDK6, PIG7/LITAF, NOXA, BCL6, INK4c/P18 and BIM) were selected for Western blot analysis in the B-NHL cell lines and biopsies from patients with B-NHL. Cellular proteins were extracted with a buffer containing protease inhibitors (1% aprotinin, 2 mM of phenylmethylsulfonyl fluoride, and 10 µg/ml leupeptin) and a phosphatase inhibitor (2 mM of sodium orthovanadate). Equal amounts of protein from each sample (50 µg) were separated on SDS-PAGE gels, and electrotransfered to nitrocellulose membranes. Finally, membranes were incubated with primary antibodies followed by secondary antibodies conjugated to horseradish peroxidase, which was detected by chemiluminescence (Pierce, Rockford, IL). The following proteins were analyzed: CDK6 and PIG7/LITAF (BD Biosciences, San Diego, CA); NOXA (Oncogene Research Products, Boston, MA); BIM (Stressgen, Canada); INK4c/P18 (Santa Cruz Biotechnology, Santa Cruz, CA, US) and BCL6 (DakoCytomation, Denmark). To evaluate equal protein transfer, detection of Actin (Oncogene Research Products, Boston, MA), β-tubulin (SIGMA, Saint Louis, M) or staining with Ponceau S (Sigma-Aldrich) were performed. Protein extracts from B-cells obtained from two non-tumoral tonsils were also analyzed.

MUTATION ANALYSIS OF *NOXA*, *PIG7/LITAF*, *INK4C/P18* AND *BIM*. For mutational analysis of *NOXA*, genomic DNA was extracted from the 48 cell lines, biopsy samples from 106 patients with different B-NHL subtypes and 50 peripheral blood samples from healthy donors. Sets of primers were designed to amplify the coding region, including each splicing site and 650 bp of the promoter, which included the possible P53 response element. For mutational analysis of

PIG7/LITAF and *BIM*, the entire coding region, and each splicing site were amplified in 48 cell lines and 15 patients with different B-NHL subtypes. For mutational analysis of *INK4c/P18*, the coding region was analyzed in the B-NHL cell lines as well as in 20 mantle cell lymphoma biopsies. PCR products were directly sequenced by using an ABI 3730 Genetic Analyzer sequencer (Applied Biosystems). *NOXA* gene sequence changes in B-NHL cell lines and patient samples; the nucleotide positions of NOXA are based on GenBank accession sequence NM_021127. The nucleotide positions of *PIG7/LITAF* are based on GenBank accesion sequence NM_004862, *BIM* on GenBank accesion sequence NM_138621 and *INK4c/P18* on GenBank accesion sequence NM_001262.

METHYLATION ANALYSIS OF *NOXA, INK4C/P18, PIG7/LITAF* AND *BIM* PROMOTERS. One µg of genomic DNA was treated with bisulfite using the CpGenomic™ DNA Modification Kit (Intergen Company, Purchase, NY). Sequence primers for the MSP analysis were designed in the 5' unstranslated region CpG island of the published sequences near translation start site. CpGenome Universal Methylated DNA (Serogicals Corporation) bisulfite-modified was used as a positive control. To evaluate demethylation, cells were treated with 4µM of the demethylating agent 5-aza-2′-deoxycitidine (Sigma); after incubation of 96 hours, cells were harvested for MSP, RT-PCR and Western blotting. For sequencing analysis, both *PIG7/LITAF* and *BIM* promoters were amplified by nested-PCR after bisulfite modification. Amplification products obtained in the second PCR reaction, were subcloned into pCR® 4-TOPO® plasmid using TOPO TA Cloning® Kit for Sequencing (Invitrogen Life Technologies, Paisley, UK) and transformed into Escherichia coli according to the manufacturer's recommendations. Colonies with recombinant plasmids containing the described PCR products were screened by digestion with *Eco*R I (Amersham Biosciences, Buckinghamshire, UK). Candidate plasmid clones were sequenced. Primers for delineation homozygous deletions, genomic sequencing, QRT-PCR, methylation specific PCR and sequencing after sodium bisulfite are shown in Supplemental Table S1

PS341 SENSITIVITY ASSAYS. Exponentially growing cells were plated at 1 x 10^6 cells/mL of RPMI medium in 24-well microtiter plates. The proteosome inhibitors PS341 (bortezomib) at concentrations of 10 and 100 nM and MG132 at 1000nM were added. After 6, 24 and 48 hours, apoptotic cells were quantified by staining with fluorescein isothiocyanate (FITC)-conjugated Annexin V and propidium iodide according to the manufacturer´s instructions (BD Pharmingen). Cell fluorescence was detected on a FACScalibur (Becton Dickinson). A minimum of 10.000 cells were acquired and analyzed using Cell Quest analysis software. All experiments were performed at least in triplicate.

TISSUE MICROARRAY STUDY OF B-NHL PATIENT SAMPLES: Pretreatment samples from 367 patients with B-NHL were analyzed using immunohistochemistry (IHC) on tissue microarrays (TMA) using a Tissue Arrayer device (Beecher Instruments, MD) as previously described.[21] Duplicated cylinders from follicular lymphoma (72 cases), mantle cell lymphoma (103 cases), diffuse large B-cell lymphoma (67 cases), splenic marginal zone lymphoma (77 cases), and B-cell chronic lymphocytic leukemia (48 cases) were included. Antibodies for NOXA, CD10, BCL2, MUM1, BCL6, LITAF, INK4c/P18 and BIM were used. Informed consent was obtained from each subject or subject's guardian. Human investigations were performed after approval by an institutional review board on scientific and ethical affairs.

RESULTS

HIGH RESOLUTION ANALYSIS OF B-NHL GENOMES

We performed genome-wide scanning for DNA copy number changes in 48 B-NHL cell lines using high-resolution array CGH (Supplemental Figure S1 and Supplemental Table S2). Eighty-eight high-level amplification events (defined by $\geq$ 4 fold DNA copy number increase) were detected, ranging from 4 to 11 fold increase and affecting 46 different chromosomal regions (Supplemental Table S3). In addition to high-level amplifications, the most common regions of low-level genomic over-representation were detected at chromosome bands 7q21.13-q21.3 (25 of 48 cell lines, 52%), 7q22.1 (48%), 7p11.2-p22.3 (44%), 8q24.1 (42%), 13q31.3-q32.3 (38%), 1q21.2-q25.1 (31-33%), 12q13.13 (29%), 18q21.1-q21.32 (27%) and Xq26.3-q28 (27%). Array CGH delineated the most frequent heterozygous genomic losses at bands 9p21.3-p22.1 (18 of 48 cell lines, 38%), 8p21.3 (29%), 17p13.1-p13.3 (29%), 17p13.1-q11.2 (27%), 11q24.2-q25 (25%) and 6q23.2-q24.1 (23%) (Supplemental Figure 2). In addition, twenty homozygous deletions involving seven different chromosome areas were identified (Table 1).

Then we applied gene expression profiling to the cell lines and searched for genes located within areas of genomic aberration that presented deregulated expression. To validate our strategy, we sought to identify critical oncogenes known to be recurrently amplified in lymphoma, most of which presented convergent high-level amplification and elevated expression in the B-NHL cell lines.[3,4,7] As representative examples, *BCL2* at chromosome 18q21.3, *BCL6* (3q27.3), *REL* and *BCL11A* (both in 2p16) and *CDK4* (12q14.1) genes, were consistently over-expressed in cell lines with respective high-level amplification (Supplemental Figure S3).

HOMOZYGOUS DELETIONS LOCALIZE POTENTIAL TUMOR SUPPRESSOR GENES

Next, we explored whether coupled analysis of gene expression and DNA copy number variation might identify candidate tumor suppressor genes by pinpointing transcripts with reduced expression related to homozygous losses. Array CGH detected twenty homozygous deletions involving seven different chromosome regions, that were confirmed by PCR analysis of BAC/PAC sequences and/or contained genes. These deletions ranged in size from 6 kb to 2 Mb (Table 1). The most frequent homozygous loss encompassed chromosome band 9p21.3 at the *INK4/ARF* locus in eight B-NHL cell lines of different origins. In the Burkitt lymphoma cell line P32, homozygous loss of 3p14.2 comprised the tumor suppressor gene *FHIT*.[22] Both are well known tumor suppressor genes involved in B-NHL pathogenesis, which indicated that our strategy might represent a valid approach for localizing novel tumor suppressor genes.

The P53-inducible gene *PIG7/LITAF* is silenced by homozygous deletion and promoter methylation in B-cell lymphoma. In the Karpas 1106 cell line derived from a patient with primary mediastinal B-cell lymphoma, we identified homozygous deletion of chromosome 16p13.13. This deletion included *PIG7/LITAF* and *SOCS1* genes, both of which showed null expression in the cDNA microarrays. Interestingly, bi-allelic mutation of *SOCS1* was recently reported specifically in patients with primary mediastinal B-cell lymphoma.[23] In addition, *PIG7/LITAF* was also considered as a candidate tumor suppressor gene, because of its *P53*-inducibility and capability to regulate apoptosis.[24,25] We performed mutational screening of *PIG7/LITAF* coding sequences in the cell lines and primary B-NHL tumors, but no pathogenic mutations were identified. Expression analysis of PIG7/LITAF by QRT-PCR and Western blot showed that PIG7/LITAF was highly expressed in non-tumoral tonsil and spleen samples, presenting comparable levels with mantle cell lymphoma cells, whereas its expression was much lower in germinal-center derived lymphomas (Figure 1A). Notably, expression of PIG7/LITAF was

inversely correlated with BCL6 expression in normal germinal center cells as well as in most of the examined cell lines at the RNA and protein levels (Figure 1B,1C,1D). A recent report suggested that the proto-oncogene *BCL6* may repress PIG7/LITAF through the transcription factor MIZ-1 in germinal center B-cells.[26] To investigate the possible pathologic mechanism responsible for the decreased expression of PIG7/LITAF in some lymphoma subsets, we analyzed promoter methylation of *PIG7/LITAF*. Five of 37 cell lines (14%) and 10 of 80 B-NHL biopsies (13%) showed promoter methylation (Figure 2A and 2B). Remarkably, PIG7/LITAF silencing was observed in diffuse large B cell lymphoma (9 cases) and Burkitt lymphoma (6 cases). A detailed mapping of CpG-methylation of the promoter by bisulfite genomic sequencing confirmed these data (Figure 2C). Methylation of *PIG7/LITAF* however was not observed in normal B-cells from spleen, blood or tonsils (Figure 2C and data not shown). Treatment with Aza induced re-expression of PIG7/LITAF in methylated cell lines (Figure 2A). IHC on tissue microarrays from 48 patient with diffuse large B cell lymphoma biopsies confirmed the opposite expression of PIG7/LITAF and BCL6 in both germinal-center diffuse large B cell lymphoma (11 of 24 cases were PIG7/LITAF- / BCL6+, 46%) and non-germinal diffuse large B cell lymphoma (10 of 24 cases were PIG7/LITAF- / BCL6+, 42%) (Figure 1D). Our data indicate that PIG7/LITAF may result inactivated by promoter methylation in a subset of diffuse large B cell lymphoma and Burkitt lymphoma.

The pro-apoptotic protein BIM is silenced by different genetic and epigenetic mechanisms in various B-NHL subtypes. Another region of recurrent genomic loss in 2q13-q21 containing *BIM* gene was observed in seven cell lines of different origins. Using array-based CGH, Tagawa *et al.* recently reported homozygous deletion of *BIM* in mantle cell lymphoma.[27] We screened for homozygous deletion of *BIM* gene and identified five mantle-cell lymphoma cell lines (UPN1, SP49, SP53, JEKO1 and Z138) but also the Burkitt lymphoma cell line P32 with bi-allelic loss

(Figure 3A). Overall, 5 of 12 (42%) mantle cell lymphoma cell lines showed bi-allelic deletion of *BIM*. Sequencing of genomic DNA failed to identify any sequence mutation in any other cell lines and primary biopsies. Western blot analysis, however, showed absence of expression in a large proportion of lymphomas of different origins (Figure 3B). To investigate this, we determined the methylation status of *BIM* gene promoter. In 11 of 23 examined cell lines (48%) and in 7 of 26 (27%) primary B-NHL biopsies of different origins, promoter methylation of *BIM* was identified. Methylations were more prominent in Burkitt lymphoma, where 6 of 7 cell lines examined (86%) and 5 of 10 patient biopsies (50%) presented *BIM* methylation (Figure 3C). However, this was not observed in any of the mantle cell lymphoma cell lines or patient biopsies studied. A detailed mapping of CpG-methylation of the promoter by bisulfite genomic sequencing confirmed these data (Figure 3D). *BIM* promoter methylation was correlated with loss of expression at the RNA and protein levels, and treatment with demethylating Aza restored BIM expression (Figure 3E). Immunohistochemistry (IHC) on tissue microarrays detected lack of BIM expression in 7 of 22 MCL samples (32%) (data not shown), which is consistent with the Western blot data. In summary, our data indicate that *BIM* is frequently silenced in different B-NHL subtypes through various mechanisms that include homozygous deletion in mantle cell lymphoma and promoter methylation in Burkitt lymphoma.

The *INK4c/P18* gene, a member of the INK4 family of cyclin-dependent kinase inhibitors, is preferentially silenced in mantle cell lymphoma. In two cell lines we observed that clone RP11-235B24 which maps to 1p32.3 showed a genomic value close to homozygosity; further screen with PCR identified homozygous deletion of *INK4c/P18* in two mantle cell lymphoma cell lines (UPN1 and HBL2) but not in the remaining B-NHL cell lines. (Figure 4A). Affymetrix oligonucleotide microarrays performed in MCL cell lines for genes located in 1p32.3-1p36 showed absence of INK4c/P18 (CDKN2C) expression in both cell lines (Figure 4B). Mutation screening

also identified hemizygous loss and point mutation at a critical splicing site of the remaining allele in JEKO1 cell line (Figure 4C). Western blot analysis revealed absence of protein expression in these three (UPN1, HBL2 and JEKO1) but also in most other mantle cell lymphoma cell lines, as well as in three patients with mantle cell lymphoma, whereas INK4c/P18 protein expression was observed in the majority of other B-NHL subtypes (Figure 4D). To search for other possible cause of decreased INK4c/P18 expression, we evaluated the promoter methylation status of INK4c/P18 in the cell lines. These studies did not reveal any case with hypermethylation of the gene (data not shown). To evaluate the significance of INK4c/P18 inactivation in patients with MCL, we performed IHC on tissue microarrays in a clinical series of patient biopsies. INK4c/P18 was strongly expressed in normal B-cells including germinal center cells, but its expression was absent in a portion of mantle cells. In 20 of the 26 evaluable cases (77%) with available clinical data, INK4c/P18 expression was undetectable. Decreased INK4c/P18 expression was correlated with unmutated *IGH* status: 4 of 6 cases (67%) showing INK4c/P18 expression presented *IGH* mutation whereas only 3 of 20 cases (15%) that did not express INK4c/P18 had a mutated *IGH* gene (p=0,02) (Figure 4E)

The pro-apoptotic BH3-only member of the BCL2 family NOXA is inactivated in B-NHL. In the Burkitt-derived cell line Elijah, a biallelic deletion of ~1,9 Mb. in band 18q21.3 was delineated (Figure 5A). This loss contained the *NOXA* gene, a BH3-only member of the *BCL2* gene family that showed null expression in Lymphochip microarrays.[28] These data were confirmed by PCR on genomic DNA, FISH, RT-PCR and QRT-PCR. Western blot analysis showed absence of expression of NOXA in Elijah and Karpas 1106 cell lines, whereas very weak expression was observed in several other cell lines (Figure 5B). Among them, three presented loss of one copy as detected in array CGH experiments (Karpas 1106, UPN1 and Namalwa). The search for inactivating mutations of the non-deleted allele revealed mutation in two: a splice site mutation

58+1G→A and a silent mutation 1-35G→A in Karpas 1106, and a missense mutation 101A→G that resulted in the amino acid change D34G in the BH3-domain in Namalwa (Figure 5C). Western blot analysis revealed that 8 of 15 primary B-NHL biopsies (53%) showed very weak expression of NOXA. Mutational screening in patient material failed to identify any inactivating mutation in NOXA open reading frame but revealed three alterations in the gene promoter sequence: 1-752C→T (2 of 106 patients), 1-653G→A (1 of 106) and 1-576A→G (1 of 106). None of these alterations was found in the B-NHL cell lines or in healthy donors. In addition, several novel and reported polymorphisms were identified. Next we investigated NOXA protein expression on biopsy samples from 367 patients with B-NHL using immunohistochemistry (IHC) on tissue microarrays. In non-tumoral tissue samples (tonsils), NOXA was shown to be expressed only in a fraction of germinal center B-cells, whereas mantle, marginal and interfollicular lymphocytes were negative (Figure 5D). NOXA protein expression was mostly cytoplasmic, but also showed occasional nuclear expression. In lymphoma samples, NOXA protein expression was found in a subset of both diffuse large B-cell lymphoma (DLBCL) (32 of 67, 48%) and follicular lymphoma (20 of 103, 19%). In the remaining B-NHL subtypes, NOXA was detected in 4 of 72 mantle cell lymphoma (5%), 4 of 77 splenic marginal zone lymphoma (5%) and 6 of 48 B-cell chronic lymphocytic leukemia (12%) samples. In the DLBCL subgroup, patient samples were also evaluated for CD10, BCL2, BCL6 and MUM1 staining and thus were classified as DLBCL of germinal center origin (n=26) and non-germinal center DLBCL subtype (n=24). NOXA expression was more common in the non-germinal center subtype (58 *vs*. 42%; p=0,16) (Figure 5D). To search for other possible cause of decreased NOXA expression, we evaluated the promoter methylation status of NOXA in the cell lines and in the patients analyzed by Western blotting. These studies did not reveal any case with hypermethylation of the gene (data not shown). Overall, our data indicate that the reduced expression of NOXA in non-germinal center-derived DLBCL possibly reflects the lower expression of NOXA in the normal cell counterpart. NOXA is a

critical mediator of the apoptotic responses induced by P53 and other agents.[28] Furthermore, it was recently reported that proteasome inhibitors trigger NOXA-mediated apoptosis in melanoma and mantle cell lymphoma.[29,30] To test this hypothesis in other B-NHL subtypes, we incubated a variety of B-cell lymphoma lines with and without *NOXA* mutation and with different levels of protein expression, with the proteasome inhibitor Bortezomib (PS-341). After 48 h of bortezomib exposure, there were no clear differences in either induction of apoptosis or apoptotic rate (Figure 5E) in the B-NHL cell lines with or without NOXA inactivation. These data suggest that in contrast to previous reports, NOXA may not be of pivotal importance in triggering proteasome inhibitor-induced apoptosis in B-cell lymphomas other than mantle cell lymphoma.[30]

Novel homozygous deletion of 4q35.1 results in *ARGBP2* and *SNX25* truncation. Another region of homozygous deletion included band 4q35.1 in the Burkitt lymphoma cell line Elijah. This deletion was caused by the complete loss of one chromosome 4 and an interstitial deletion of the remaining chromosome. Delineation of the deleted segment by "PCR walking" revealed a loss of 251 kb between two genes on chromosome 4q35.1, *ARGBP2/SORBS2* centromerically and *SNX25* telomerically (Figure 6A). The former gene encodes an adapter protein that interacts directly with ABL via SH3 domains in the carboxy terminus and may link ABL with the actin cytoskeleton. *ARGBP2* is broadly expressed in normal and malignant tissues, whereas the more telomeric gene, *SNX25* appears to be B-cell specific. The two genes are in opposite transcriptional orientation. The deletion reakpoints fell within the carboxy-terminal coding regions of both genes; the *ARGBP2* breakpoint fell within the intron immediately telomeric to exon 30, whilst the *SNX25* breakpoint fell within an intron, centromeric to exon 15 (Figure 6B). 3' RACE experiments showed splicing of both *ARGBP2* and *SNX25* transcripts to splice to cryptic splice acceptor sites and exons in the opposite transcriptional orientation, resulting in the introduction of premature stop codons in both genes (Figures 6C and 6D). As a consequence of the fusion,

ARGBP2 loses a crucial COOH terminal domain that may interfere with its binding to ABL .[31] However, we did not detect a similar gene fusion or a homozygous deletion in 4q35.1 in the remaining B-NHL cell lines nor in a subset of primary B-NHL biopsies (data not shown). The possible functional consequences of the truncation of the COOH terminal domain in SNX25 are currently unclear, and whether this novel mechanism of gene inactivation is also observed in other homozygous deletions in cancer is currently under investigation.

DISCUSSION

We report that array CGH combined with gene expression profiling represents a valid strategy for localizing tumor suppressor genes in regions of homozygous loss in B-cell lymphoma. In a recent survey of homozygous deletions in 636 cancer cell lines, mostly of non-lymphoid origin,[22] the gene count within homozygous deletions was low compared with the rest of the genome and many of these areas did not contain coding genes. In contrast, all homozygous deletions identified in our B-NHL cell lines included coding genes. The number of homozygous losses in the B-NHL cell line panel (20 in 48 cases, 0,42 per cell line) was similar to that found in the carcinoma cell lines (281 homozygous deletions in 636 cancer cell lines, 0,44 per cell line). These data indicate that the integrity of the B-cell lymphoma and carcinoma genomes are equally unstable, but the nature of the homozygous losses may be different. In lymphoma, bi-allelic loss results in the inactivation of coding tumor suppressor genes probably implicated in tumor development and progression whereas the low density or absence of coding genes within regions of homozygous deletion in the carcinoma cell lines raises the possibility that other types of transcript may be the target for homozygous deletion.[22] An attractive hypothesis is that homozygous deletions in gene-free regions confer positive selective advantage by deleting regulatory regions or non-coding microRNAs that are necessary for control of the expression of recessive or dominant cancer genes.

Our study pointed out several candidate tumor suppressor genes inactivated by bi-allelic deletion. Further investigation revealed that only a fraction of cell lines and primary biopsies presented inactivation of these genes by point mutation or intragenic deletion, but instead some of these genes were frequently silenced at the epigenetic level by promoter methylation. Notably, the pattern of genetic and epigenetic inactivation for these genes was different and varied among the

B-NHL subtypes. Thus, mantle cell lymphomas showed frequent homozygous deletion of *BIM* gene whereas it was commonly silenced by promoter methylation in Burkitt lymphoma and in diffuse large B-cell lymphoma. As *BIM* was recently reported to be the target of *MYC* mutants but not of wild-type translocated *MYC* in a Burkitt-lymphoma mouse model,[32] we may speculate that tumor-derived *MYC* mutants may silence *BIM* expression through active recruitment of DNA methyltransferase corepressor, as has been reported for $P21^{Cip1}$ gene.[33] On the contrary, BIM silencing in mantle cell lymphoma seems to follow a different mechanism orchestrated by the cyclin D1 activation as a consequence of the t(11;14) translocation, probably in cooperation with the common DNA repair defects that are observed in this lymphoma subtype.[27,34] Our data reinforce the role of BIM as a relatively specific suppressor of tumorigenesis inactivated through different mechanisms in lymphoma.[32,35]

We also identified inactivation of the cyclin-dependent kinase inhibitor *INK4c/P18* in MCL. Because unmutated *IGH* has been associated with aggressive clinical evolution of MCL,[36] inactivation of *INK4c/P18* gene by bi-allelic mutation may be associated with aggressive MCL. We may also suggest that the decreased expression of INK4c/P18 observed in *IGH*-ummutated cells may indicate that these tumors originated from mantle cells that do not express INK4c/P18, whereas tumors expressing INK4c/P18 originated from *IGH*-mutated mantle cells that express INK4c/P18.

One of the most prominent candidate tumor suppressor genes detected in our study is *PIG7/LITAF*, a P53 inducible gene that is also a LPS-induced TNF-alpha transcription factor.[24,25] In addition, mutations of *PIG7/LITAF* have been reported as the causative mechanism of Charcot-marie-Tooth disease type 1C.[37] However, mutation screening of *PIG7/LITAF* coding sequences in the B-NHL cell lines and primary B-NHL tumors did not identify any clear

pathogenic mutation. The possible implication of *PIG7/LITAF* as a suppressor gene could be related to its P53-inducibility and regulation of apoptosis. Additional support for the involvement of *PIG7/LITAF* in lymphoma comes from a recent report that suggested that the proto-oncogene *BCL6* may repress *PIG7/LITAF* through the transcription factor MIZ-1 in germinal B-cells.[26] Supporting this hypothesis, we have observed an inverse correlation of *PIG7/LITAF* and *BCL6* expression in most of the examined cell lines at the RNA and protein levels. Our data strongly suggest that *PIG7/LITAF* may have suppressor activity in diffuse large B-cell lymphoma and Burkitt lymphoma. We hypothesize that mutant BCL6 may silence PIG7/LITAF by inducing its promoter methylation. The cell lines described here are being used to functionally characterize PIG7/LITAF and its role in B-cell malignancies.

Our data also pinpointed additional genes targeted by homozygous deletion in lymphoma. The *NOXA* gene was found inactivated by homozygous deletion and point mutation in different lymphoma cell lines. In addition, a missense mutation in the conserved BH3-domain was also identified. However, we did not identify similar mutations nor promoter methylation in lymphoma primary samples. Instead, we observed decreased NOXA protein expression in patient with non-germinal diffuse large B-cell lymphoma, possibly reflecting the low expression of NOXA in their the normal cell counterpart. A recent report by Perez-Galan *et al*. indicated that in mantle cell lymphoma, NOXA depletion by RNA interference markedly decreased sensitivity to bortezomib, pointing to this protein as a key mediator between proteasome inhibition and mitochondrial depolarization in this lymphoma subtype. After incubation of different B-NHl lymphoma cell lines with different levels of NOXA with bortezomib, we did not observe differences in apoptosis, therefore not confirming the pivotal importance of NOXA in triggering proteasome-induced apoptosis in B-cell lymphomas other than mantle cell lymphoma.[30]

In summary, our combined approach has shown the extent to which DNA copy number variation influences the deregulation of gene expression in B-NHL. We demonstrate that array CGH combined with gene expression profiling may provide a rational for discovering tumor suppressor genes in regions of homozygous loss. These target genes show different genetic and epigenetic mechanisms of inactivation that substantially vary among the B-NHL subtypes. Similar screens for tumor suppressor genes can be extended to the analysis of other cancers.

TABLES

Table 1: Molecular delineation of seven regions of homozygous genomic loss in B-NHL. Identification of putative tumor suppressor genes in B-NHL

[a] Map positions and cytogenetic locations are based on data available through the UCSC genome browser (May 2004 freeze).

[b] Molecular delineation of regions of homozygous genomic loss was performed using array CGH, FISH and PCR of genomic DNA. For delineation of homozygous deletion borders, the more open positions of deleted BACs, have been used. The homozygous deletions of *BIM* and *CDKN2C* were demonstrated only by PCR.

[c] In UPN1 cell line, partial homozygous deletion of BIM locus was demonstrated by PCR of genomic DNA.

[d] REC1, Z138, K353, DOHH2, G452 and 380 cell lines showed only one deleted BAC, CTB-65D18, sized 0.1 Mb (9p21.3). OZ and MD903 cell lines showed a region of deletion of 5.6 Mb (9p21.3-9p21.2), from CTB-65D18 to RP11-235F7.

[e] In MD903 cell line, partial homozygous deletion of CTB-65D18 including the INK4/ARF locus was demonstrated by PCR of genomic DNA.

[f] Homozygous deletion of BACs not included in the array was demonstrated by FISH.

Table 1

REGION OF CROMOSOME DELETION [a]	CELL LINES	DELETED BACS	SIZE OF REGION OF DELETION (Mb) [a, b]	PUTATIVE TARGET GENES WITHIN REGION OF DELETION
1p32.3	HBL2, UPN1	-	0.006-0.690	*INK4c/P18*
2q13	UPN1 [c], SP49, SP53, JEKO1, Z-138, P32	-	0.043-0.751	*BIM*
3p14.2	P32	RP11-94D19	0.2	*FHIT*
4q35.1	ELIJAH	RP11-203L17, RP11-159A22	0.25	*ARGBP2, SNX25*
9p21.3-9p21.2 [d]	REC1, Z-138, OZ, Karpas 353, DOHH2, MD903 [e], Granta 452, 380	CTB-65D18, RP11-33015, RP11-85J15, RP11-55P9, CTD-2170E19, RP11-235F7	0.1-5.6	*INK4/ARF*
16p13.13	K1106	RP11-396B14 [f], RP11-49M6, RP11-547D14 [f]	0.6	*SOCS1, LITAF*
18q21.32-18q21.33	ELIJAH	RP11-12J12, RP11-40D15, RP11-15C15	2.0	*NOXA*

FIGURES

FIGURE 1. Identification of homozygous deletion and expression of *PIG7/LITAF*

A Real time RT-PCR analysis of PIG7/LITAF expression in samples from tonsil and spleen and in B-NHL cell lines (10 Mantle cell lymphoma cell lines; 11 diffuse large B cell lymphoma cell lines with t(14:18); 3 diffuse large B cell lymphoma cell lines lacking t(14;18) and 6 Burkitt lymphoma cell lines. Data shown are the relative gene expression levels normalized with *GAPDH*; bars indicate standard deviations. The results are derived from 3 independent experiments. MCL, mantle cell lymphoma, DLBCL, diffuse large B cell lymphoma, BL Burkitt lymphoma.

B. Affymetrix oligonucleotide microarrays and Western blot analyses of PIG7/LITAF and BCL6 in mantle cell lymphoma cell lines. KHM10B cell line was used as a positive control for BCL6 expression.

C. Lymphochip cDNA microarrays and Western blot analyses of PIG7/LITAF and BCL6 in B-NHL cell lines of different origins.

D. Immunohistochemistry analysis for PIG7/LITAF and BCL6 protein on tissue microarrays. In non-tumoral tissue samples (tonsils), PIG7/LITAF expression was cytoplasmatic and was shown to be expressed mostly in mantle, marginal and interfollicular lymphocytes whereas BCL6 was shown to be expressed in germinal center B cells.

FIGURE 2. Promoter methylation of *PIG7/LITAF.*

A. Methylation-specific PCR (MSP), Quantitative RT-PCR and Western blot analysis of PIG7/LITAF in RL and SCl1 cell lines before and after treatment with 4μM of 5-Aza-2'-deoxycitine. The treatment with demethylating Aza restored PIG7/LITAF expression at the RNA and protein levels. In the QRT-PCR data analysis, gene expression levels were normalized with *GAPDH* as an internal control; bars indicate standard deviations.

B. Methylation-specific PCR (MSP) in primary biopsies of Burkitt lymphoma. M, methylated and U, unmethylated.

C. Sequence analysis of the *PIG7/LITAF* promoter region after bisulfite modification. The black box indicates the methylated cytosine while the white box indicated the unmethylated cytosine in the dinucleotide CpG. C+ indicates methylated control 1: genomic sequence of *PIG7/LITAF* promoter region. 2: methylated sequence of the *PIG7/LITAF* promoter region after bisulfite modification and 3: unmethylated sequence of the *PIG7/LITAF* promoter region after bisulfite modification.

FIGURE 3. Identification of homozygous deletion and promoter methylation of *BIM*

A. Array CGH and genomic PCR studies of mantle cell lymphoma cell lines, showing interstitial homozygous deletion of *BIM* gene. In none of the cases, deletion of *BUB1* gene was observed.

B. Western blot analysis shows absence of expression of BIM protein in mantle cell lymphoma but also in Burkitt lymphoma cell lines and patient biopsies.

C. Methylation of *BIM* promoter was frequently detected in Burkitt lymphoma cell lines and patient biopsies as well as in a subset of B-NHL from different origins, but not in mantle cell lymphoma.

D. A detailed mapping of CpG-methylation of the promoter by bisulfite genomic sequencing confirmed previous data.

E. *BIM* promoter methylation was correlated with loss of expression at the RNA and protein levels, and treatment with demethylating Aza restored BIM expression.

FIGURE 4. Inactivation of *INK4c/P18* in mantle cell ylmphoma

A. Array CGH studies and further screen with genomic PCR identified homozygous deletion of *INK4c/P18* in two mantle cell lymphoma cell lines (UPN1 and HBL2) but not in the remaining B-NHL cell lines.

B. Affymetrix oligonucleotide microarrays performed in MCL cell lines of genes located in 1p36-1p32.3 showed absence of CDKN2C expression in both cell lines.

C. Mutation screening identified hemizygous loss and point mutation of *INK4c/P18* at a critical splicing site of the remaining allele in JEKO1 cell line, which correlated with absence of P18 expression.

D. Western blot analysis revealed absence of protein expression in these three cell lines (UPN1, HBL2 and JEKO1) but also in the majority of other mantle cell lymphoma cell lines, and in three patients with mantle cell lymphoma, whereas INK4c/P18 protein expression was observed in the majority of other B-NHL subtypes.

E. IHC on tissue microarrays revealed absence of expression of INK4c/P18 in mantle cell lymphoma with IGH ummutated status.

FIGURE 5. Genomic and proteomic analysis of NOXA in B-NHL

A. Array CGH analysis of ELIJAH cells shows homozygous deletion of chromosome band 18q21.3. Within the region, NOXA gene expression shows null expression in the Lymphochip microarrays.

B. Western blot and QRT-PCR analyses show expression variation of NOXA in different B-NHL cell lines; in ELIJAH, NOXA protein expression is absent according to DNA and RNA data.

C. *NOXA* gene sequence changes in B-NHL cell lines; the nucleotide positions of NOXA are based on GenBank accession sequence NM_021127. Sequencing analysis of the non-deleted

alleles reveals a splice site mutation in Karpas 1106 and a misense mutation in the BH3-domain in Namalwa.

D. Immunohistochemistry analysis for NOXA protein on tissue microarrays from 367 biopsies from patients with different B-NHL. In tonsils, NOXA was shown to be expressed only in a fraction of germinal center B-cells, whereas mantle, marginal and interfollicular lymphocytes were negative. In lymphoma samples, NOXA protein expression was restricted to diffuse large B-cell lymphoma (32 of 67, 48%) and in a subset of follicular lymphoma (20 of 103, 19%), whereas mantle cell lymphoma, splenic marginal zone lymphoma and B-cell chronic lymphocytic leukemia samples were mostly negative.

E. Proteasome inhibitor, bortezomib (PS-341) in B-NHL cell lines with and without NOXA mutation. Cell lines were incubated for 24 and 48 h with increasing concentrations of bortezomib. Apoptosis was calculated by measuring phosphatidylserine (PS) externalisation as determined using Annexin V. The results correlated with loss of mitochondrial membrane potential (data not shown). Both the induction and rate of apoptosis was comparable between all the cell lines, irrespective of the presence of genetic alterations in NOXA.

FIGURE 6. Homozygous deletion of 4q35.1.

A. In the Elijah cell line, delineation of the deleted segment in 4q35.1 revealed a small deletion of 251 kb between the potential candidates genes *ARGBP2* and *SNX25*, both of which resulted truncated in a cryptic fusion between *SNX25* exon 15 and *ARGBP2* intron, and between ARGBP2 exon 18 and SNX25 intron.

B, **C.** Both genes splice to cryptic splice acceptor sites in the opposite transcriptional orientation. As a consequence of the deletion, ARGBP2 loses a crucial COOH terminal domain that may interfere with its binding to CBL and SNX25 also results in the truncation of the COOH terminal domain. Deletion of *ALP* gene, mapped between *ARGBP2* and *SNX25*, is also detected.

D. Truncated SNX25 mRNA is expressed using RT-PCR.

SUPPLEMENTAL WEB TABLES

SUPPLEMENTAL TABLE S1. Primers for QRT-PCR, sequence analysis and MSP. Primers and QRT-PCR measurement of *CDK6* and *NOXA* genes in the B-NHL cell lines, and primers for genomic sequencing and methylation analysis using MSP for *PIG7/LITAF, BIM, INK4c/P18* and *NOXA* are shown.

SUPPLEMENTAL TABLE S2. Full karyotype and standard CGH description of 25 B-NHLcell lines. We performed genome-wide scanning for DNA copy number changes in 48 B-NHL cell lines using an array CGH method that covers the genome with a 1.4 Mb resolution (Figure 1). To assess sensitivity and resolution, array CGH patterns were compared to those of standard CGH to chromosomes (s-CGH) and to the cytogenetic analysis in 25 selected cell lines. On average, each cell line displayed 20 genomic changes in array CGH analysis (range, 4-35), comprising roughly equal numbers of gains and losses. In the 25 selected cell lines, s-CGH and cytogenetic analysis revealed a lower number of aberrations than in array CGH studies: mean number of abnormalities per case were 13 (range 1-25) and 12 (range, 2-20) in s-CGH and G-banding studies, respectively. Of the total of 70 genomic amplifications revealed by array CGH in the 25 cell lines, only 22 (31%) were detected by s-CGH. Similarly, among 230 genomic losses detected by array CGH, only 95 (41%) were revealed by s-CGH. Thus, array CGH provided a more accurate quantitative and qualitative portrait of the DNA copy number changes in the B-NHL cell lines. To evaluate reproducibility of array CGH experiments, same aliquots from SCI1, PR1, OCI-Ly8 and Z138 cell lines were analyzed twice. In the comparative analysis, only 14 clone pairs (range 4-33) from each of the paired tumors (representing the 0,7% of the probes that were successfully hybridized) from the different array CGH experiments showed discordant values (defined as differences in log2 value exceeding 0,3). In summary, array CGH was more sensitive

than conventional CGH, and was a highly reproducible method for the scanning of lymphoma genomes.

SUPPLEMENTAL TABLE S3. Representation of amplification sites and genes targeted with elevated expression in B-NHL.

[a] Map positions and cytogenetic locations are based on data available through the University of California Santa Cruz genome browser (May 2004 freeze). [b] For amplicon borders, the more extern positions of amplified clones has been used. [c] Because abnormal clones that delineated the amplicon borders have been excluded in the May 2004 freeze of the UCSC genome browser, the closest positions of neighboring unamplified clones have been used. [d] Candidate genes with elevated expression are mapped to amplified regions delineated by the closest positions of neighboring unamplified clones.

SUPPLEMENTAL FIGURES

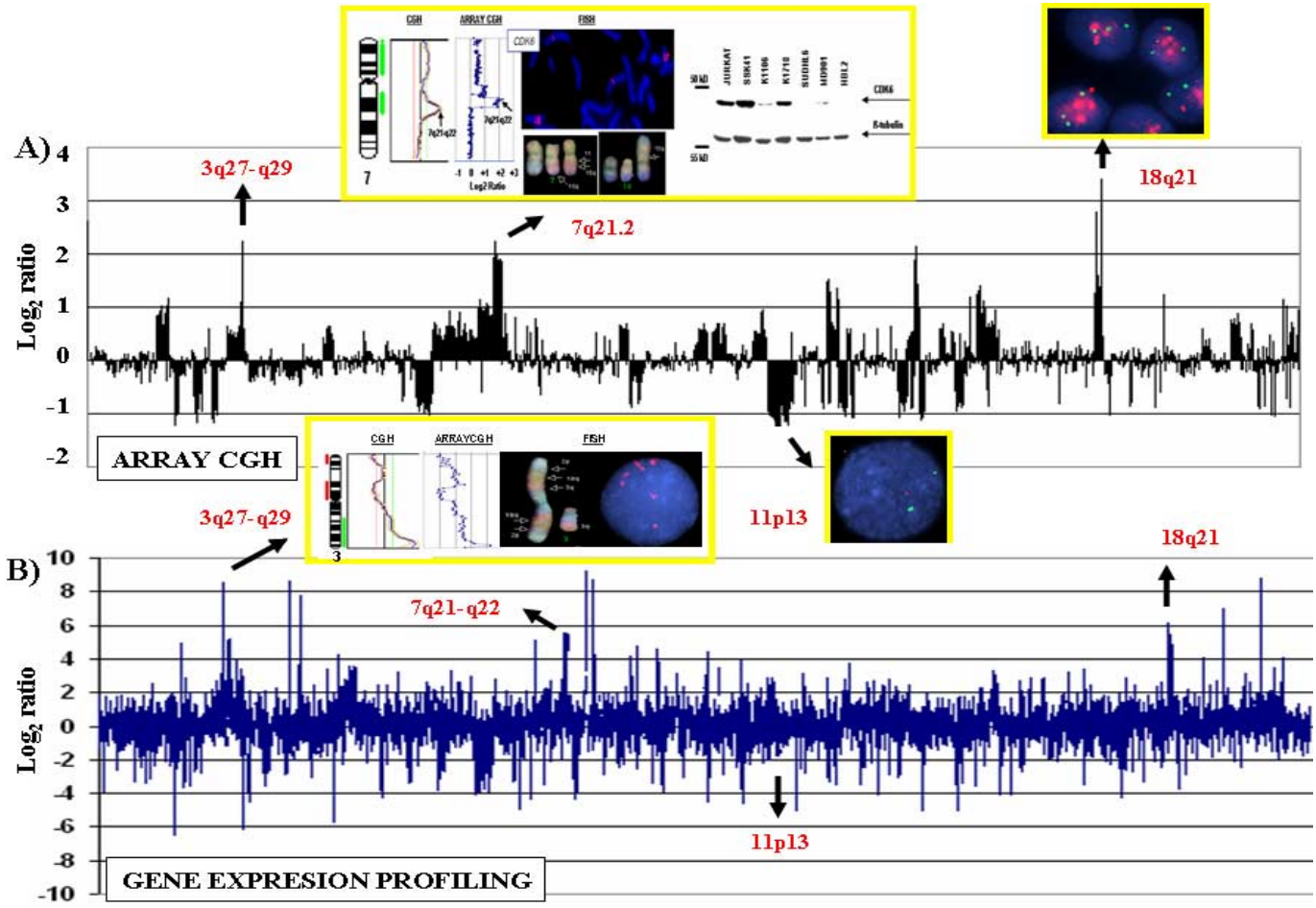

SUPPLEMENTAL FIGURE S1. Genome-wide array CGH and cDNA microarray analyses of B-NHL.

Genome-wide DNA and RNA copy number variation in the SSK-41 cell line using array CGH (A) and gene expression profiling (B) across the genome; probes were ordered according to their cytogenetic position from 1p telomere to Xq telomere. Individual amplifications of 3q27-q29, 7q21-q22 and 18q21, and genomic deletion of 11p13, were confirmed, as shown, using s-CGH, FISH and color cytogenetic analyses. The upper inset shows the partial s-CGH and array CGH analyses of the SSK41 cell line, demonstrating amplification of 7q21-q22 involving *CDK6* gene, which also showed deregulated expression in gene expression analysis. Cytogenetic analysis

showed a der(7)t(7;15)(q21;q15), +der(7)t(7;11;15)(q21;q21-q22;q15), del(10)(p12), +der(10)t(7;10)(q10;p10). FISH studies using a BAC probe containing the gene showed *CDK6* amplification in the SSK41 cell line. Western blot analyses revealed CDK6 over-expression in SSK41 cell line as well in Karpas 1718, both derived from patients with marginal zone lymphoma. Other cell lines with gain of 7q derived from other B-NHL subtypes did not show elevated expression of CDK6.

We performed genome-wide scanning for DNA copy number changes in 48 B-NHL cell lines using high-resolution array CGH. To assess sensitivity and resolution, array CGH patterns were compared to those of standard CGH (s-CGH) and to the cytogenetic analysis in 25 selected cell lines. On average, each cell line displayed 20 genomic changes in array CGH analysis (range, 4-35), comprising roughly equal numbers of gains and losses. s-CGH and cytogenetic analysis revealed a lower number of aberrations than array CGH: mean number of abnormalities per cell line were 13 (range 1-25) and 12 (range, 2-20) in s-CGH and G-banding studies, respectively. Of the total of 70 genomic amplifications revealed by array CGH in 25 cell lines, only 22 (31%) were detected by s-CGH. Similarly, among 230 genomic losses detected by array CGH in 25 cell lines, only 95 (41%) were revealed by s-CGH. These data indicate that array CGH provided a more accurate portrait of the DNA copy number changes in the B-NHL cell lines. To evaluate reproducibility of array CGH, the same aliquots from SCI1, PR1, OCI-Ly8 and Z138 cell lines were analyzed in duplicate. Only 14 clone pairs (range 4-33) from each of the paired tumors (representing the 0,7% of the probes that were successfully hybridized) from the different array CGH experiments showed discordant values (defined as differences in log2 value exceeding 0,3), confirming the reproducibility of the array CGH method.

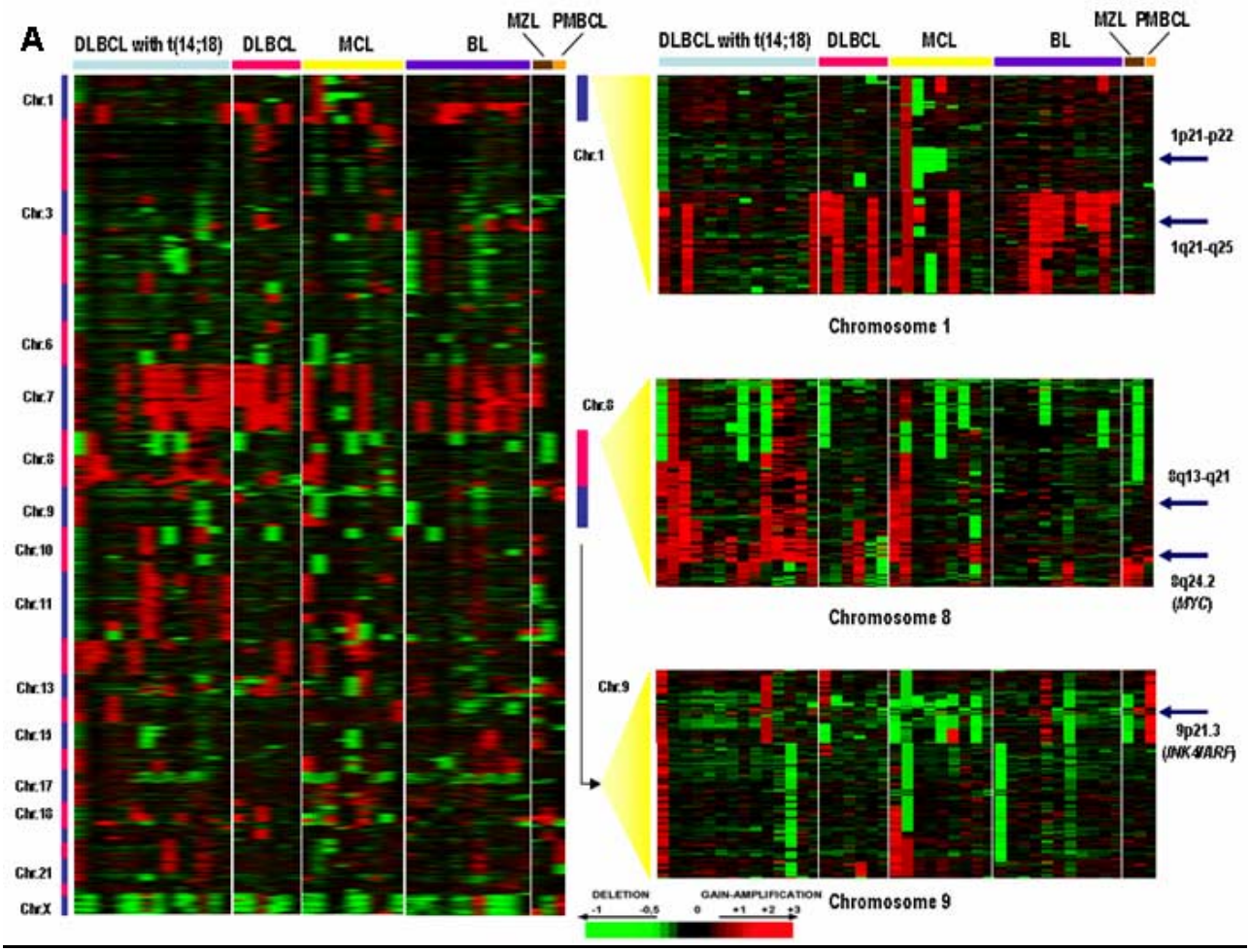

SUPPLEMENTAL FIGURE S2. Array CGH analysis of the different B-NHL subtypes

Left, array CGH profile of different B-NHL subgroups. DLBCL indicates diffuse large B-cell lymphoma; MCL, mantle cell lymphoma; BL, Burkitt lymphoma; MZL, marginal zone lymphoma and PMBCL, primary mediastinal B-cell lymphoma. Right, array CGH profiles show genomic alterations that are associated with particular B-NHL subgroups: deletion of chromosome 1p21.2 only in MCL; gain of 1q21.2-q25.1 in BL; gains of 8q13-q21 and 8q24.2 (*MYC* locus) in DLBCL with the t(14;18)(q32;q21) and deletion of 9p21.3 (*INK4/ARF* locus) in MCL. Genomic gains are shown in red, genomic losses in green and regions with normal DNA copy number in black.

We investigated the association between specific genomic aberrations and the different B-NHL subtypes. The deletion of chromosome 1p21.2 was the only locus observed in only one B-NHL category, namely mantle cell lymphoma, but not in other subgroups (42% vs 0%; p=0,0005)

(Supplemental Figure S2). Some other genomic changes were correlated with the different B-NHL subgroups. These included the deletion of chromosome bands 9p21.3 at *INK4/ARF* locus (75% *vs* 25%; p=0,003) and 2q13-2q21.2 at *BIM* locus (33% *vs* 8%; p= 0,05) and the gain of 3q13.33-q21.3 (33% *vs* 3%; p=0.01) in mantle cell lymphoma; the gain of 8q24.21 (*MYC* locus) (73% *vs* 27%; p=0,004) and 11p15.2-p15.4 (33% *vs* 9%; p=0,05) in diffuse large B-cell lymphoma with the t(14;18)(q32:q21) translocation; the gain of 13q14.11 in diffuse large B-cell lymphoma without the t(14;18)(q32;q21) translocation (50% *vs* 12%; p=0,05) and the gain of 1q21.2-q23.3 (64% *vs* 22%; p=0,01) and the deletion of 17p13.1 involving *P53* (55% *vs* 22%; p=0,04) in Burkitt lymphoma. Therefore, regional genomic gains and losses showed a different distribution pattern among the B-NHL subtypes.

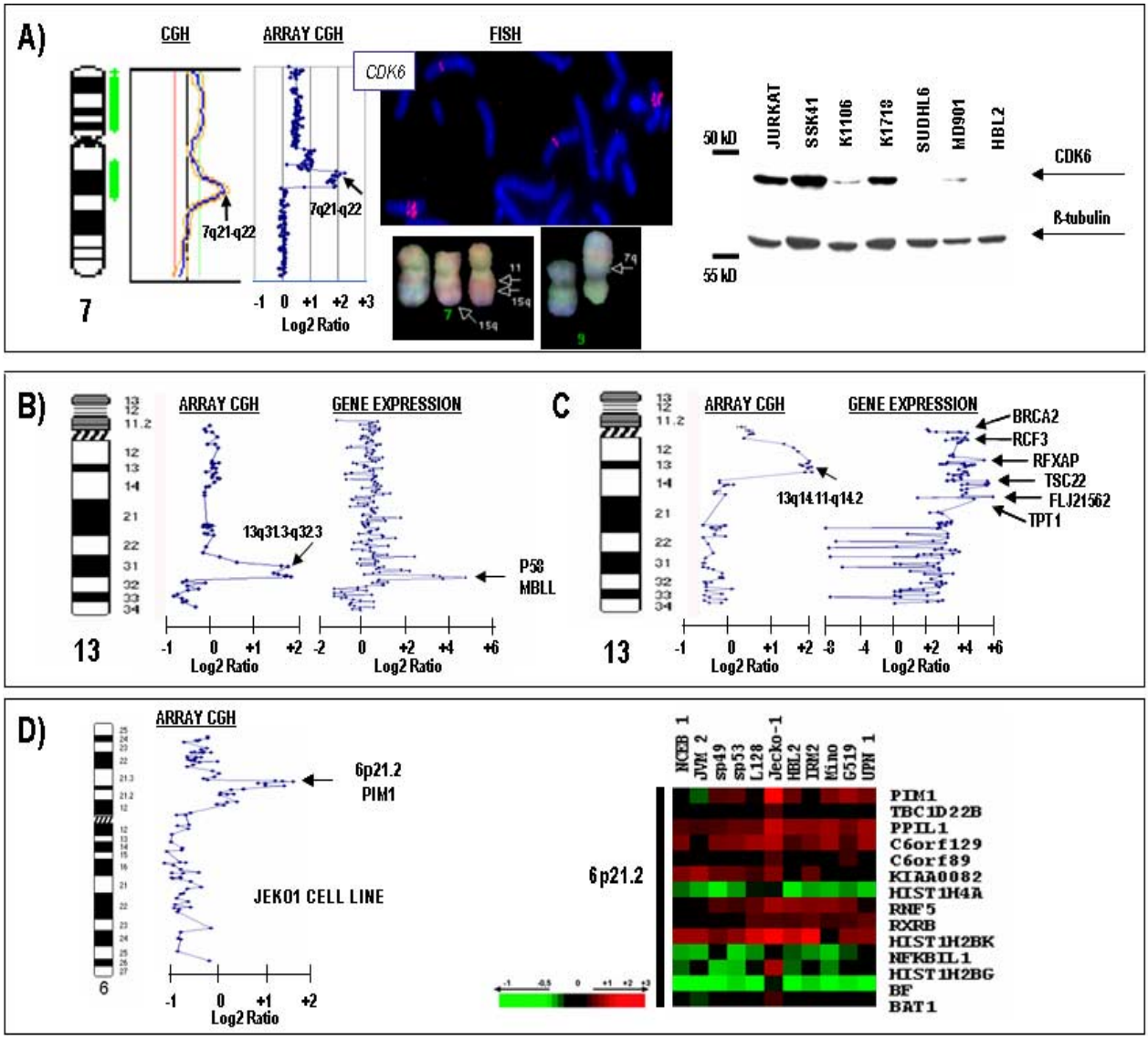

SUPPLEMENTAL FIGURE S3.

Identification of targeted oncogenes in B-NHL

A. Amplification and over-expression of *CDK6* in marginal zone lymphoma cell line SSK41. Complementary FISH, color cytogenetic and Western blot analyses are shown.

B. Amplification of different chromosome 13q segments in SSK41 (left) and MD903 (right) cell lines identified numerous genes targeted at the RNA level.

C. Amplification of 6p21.2 incolving *PIM1* in the JEKO1 mantle cell lymphoma cell line. Over-expresison of *PIM1* was detected in Lymphchip microarrays. In addition, we searched for *PIM1* expression in 11 mantle cell lymphoma cell lines using Affymetrix oligonucleotide microarrays,

being only JEKO1 the one with 6p amplicon. A number of genes across 6p21.2 showed elevated expression in JEKO1 *vs.* the remaining cell lines. Among them, *PIM1* presented higher differential expression at the RNA level.

REFERENCES

1. Willis TG, Dyer MJ. The role of immunoglobulin translocations in the pathogenesis of B-cell malignancies. Blood. 2000;96:808-822.
2. McDonnell TJ, Korsmeyer SJ. Progression from lymphoid hyperplasia to high-grade malignant lymphoma in mice transgenic for the t(14; 18). Nature. 1991;349:254-256.
3. Bea S, Ribas M, Hernandez JM, et al. Increased number of chromosomal imbalances and high-level DNA amplifications in mantle cell lymphoma are associated with blastoid variants. Blood. 1999;93:4365-4374.
4. Bentz M, Werner CA, Dohner H, et al. High incidence of chromosomal imbalances and gene amplifications in the classical follicular variant of follicle center lymphoma. Blood. 1996;88:1437-1444.
5. Rubio-Moscardo F, Climent J, Siebert R, et al. Mantle-cell lymphoma genotypes identified with CGH to BAC microarrays define a leukemic subgroup of disease and predict patient outcome. Blood. 2005;105:4445-4454.
6. Tagawa H, Suguro M, Tsuzuki S, et al. Comparison of genome profiles for identification of distinct subgroups of diffuse large B-cell lymphoma. Blood. 2005;106:1770-1777.
7. Rao PH, Houldsworth J, Dyomina K, et al. Chromosomal and gene amplification in diffuse large B-cell lymphoma. Blood. 1998;92:234-240.
8. Ishkanian AS, Malloff CA, Watson SK, et al. A tiling resolution DNA microarray with complete coverage of the human genome. Nat Genet. 2004;36:299-303.
9. Wessendorf S, Schwaenen C, Kohlhammer H, et al. Hidden gene amplifications in aggressive B-cell non-Hodgkin lymphomas detected by microarray-based comparative genomic hybridization. Oncogene. 2003;22:1425-1429.
10. Pollack JR, Sorlie T, Perou CM, et al. Microarray analysis reveals a major direct role of DNA copy number alteration in the transcriptional program of human breast tumors. Proc Natl Acad Sci U S A. 2002;99:12963-12968.
11. Tonon G, Wong KK, Maulik G, et al. High-resolution genomic profiles of human lung cancer. Proc Natl Acad Sci U S A. 2005;102:9625-9630.
12. Aguirre AJ, Brennan C, Bailey G, et al. High-resolution characterization of the pancreatic adenocarcinoma genome. Proc Natl Acad Sci U S A. 2004;101:9067-9072.
13. Martinez-Climent JA, Alizadeh AA, Segraves R, et al. Transformation of follicular lymphoma to diffuse large cell lymphoma is associated with a heterogeneous set of DNA copy number and gene expression alterations. Blood. 2003;101:3109-3117.
14. de Leeuw RJ, Davies JJ, Rosenwald A, et al. Comprehensive whole genome array CGH profiling of mantle cell lymphoma model genomes. Hum Mol Genet. 2004;13:1827-1837.
15. Albertson DG, Ylstra B, Segraves R, et al. Quantitative mapping of amplicon structure by array CGH identifies CYP24 as a candidate oncogene. Nat Genet. 2000;25:144-146.
16. Bea S, Tort F, Pinyol M, et al. BMI-1 gene amplification and overexpression in hematological malignancies occur mainly in mantle cell lymphomas. Cancer Res. 2001;61:2409-2412.
17. Sanchez-Izquierdo D, Buchonnet G, Siebert R, et al. MALT1 is deregulated by both chromosomal translocation and amplification in B-cell non-Hodgkin lymphoma. Blood. 2003;101:4539-4546.

18. Tagawa H, Karnan S, Kasugai Y, et al. MASL1, a candidate oncogene found in amplification at 8p23.1, is translocated in immunoblastic B-cell lymphoma cell line OCI-LY8. Oncogene. 2004;23:2576-2581.
19. Snijders AM, Nowak N, Segraves R, et al. Assembly of microarrays for genome-wide measurement of DNA copy number. Nat Genet. 2001;29:263-264.
20. Alizadeh AA, Eisen MB, Davis RE, et al. Distinct types of diffuse large B-cell lymphoma identified by gene expression profiling. Nature. 2000;403:503-511.
21. Garcia JF, Camacho FI, Morente M, et al. Hodgkin and Reed-Sternberg cells harbor alterations in the major tumor suppressor pathways and cell-cycle checkpoints: analyses using tissue microarrays. Blood. 2003;101:681-689.
22. Cox C, Bignell G, Greenman C, et al. A survey of homozygous deletions in human cancer genomes. Proc Natl Acad Sci U S A. 2005;102:4542-4547.
23. Melzner I, Bucur AJ, Bruderlein S, et al. Biallelic mutation of SOCS-1 impairs JAK2 degradation and sustains phospho-JAK2 action in the MedB-1 mediastinal lymphoma line. Blood. 2005;105:2535-2542.
24. Moriwaki Y, Begum NA, Kobayashi M, Matsumoto M, Toyoshima K, Seya T. Mycobacterium bovis Bacillus Calmette-Guerin and its cell wall complex induce a novel lysosomal membrane protein, SIMPLE, that bridges the missing link between lipopolysaccharide and p53-inducible gene, LITAF(PIG7), and estrogen-inducible gene, EET-1. J Biol Chem. 2001;276:23065-23076.
25. Polyak K, Xia Y, Zweier JL, Kinzler KW, Vogelstein B. A model for p53-induced apoptosis. Nature. 1997;389:300-305.
26. Phan RT, Saito M, Basso K, Niu H, Dalla-Favera R. BCL6 interacts with the transcription factor Miz-1 to suppress the cyclin-dependent kinase inhibitor p21 and cell cycle arrest in germinal center B cells. Nat Immunol. 2005.
27. Tagawa H, Karnan S, Suzuki R, et al. Genome-wide array-based CGH for mantle cell lymphoma: identification of homozygous deletions of the proapoptotic gene BIM. Oncogene. 2004.
28. Oda E, Ohki R, Murasawa H, et al. Noxa, a BH3-only member of the Bcl-2 family and candidate mediator of p53-induced apoptosis. Science. 2000;288:1053-1058.
29. Qin JZ, Ziffra J, Stennett L, et al. Proteasome inhibitors trigger NOXA-mediated apoptosis in melanoma and myeloma cells. Cancer Res. 2005;65:6282-6293.
30. Perez-Galan P, Roue G, Villamor N, Montserrat E, Campo E, Colomer D. The proteasome inhibitor bortezomib induces apoptosis in mantle-cell lymphoma through generation of ROS and Noxa activation independent of p53 status. Blood. 2006;107:257-264.
31. Yuan ZQ, Kim D, Kaneko S, et al. ArgBP2gamma interacts with Akt and p21-activated kinase-1 and promotes cell survival. J Biol Chem. 2005;280:21483-21490.
32. Hemann MT, Bric A, Teruya-Feldstein J, et al. Evasion of the p53 tumour surveillance network by tumour-derived MYC mutants. Nature. 2005;436:807-811.
33. Brenner C, Deplus R, Didelot C, et al. Myc represses transcription through recruitment of DNA methyltransferase corepressor. Embo J. 2005;24:336-346.
34. Fernandez V, Hartmann E, Ott G, Campo E, Rosenwald A. Pathogenesis of mantle-cell lymphoma: all oncogenic roads lead to dysregulation of cell cycle and DNA damage response pathways. J Clin Oncol. 2005;23:6364-6369.
35. Egle A, Harris AW, Bouillet P, Cory S. Bim is a suppressor of Myc-induced mouse B cell leukemia. Proc Natl Acad Sci U S A. 2004;101:6164-6169.
36. Orchard J, Garand R, Davis Z, et al. A subset of t(11;14) lymphoma with mantle cell features displays mutated IgVH genes and includes patients with good prognosis, nonnodal disease. Blood. 2003;101:4975-4981.

37. Street VA, Bennett CL, Goldy JD, et al. Mutation of a putative protein degradation gene LITAF/SIMPLE in Charcot-Marie-Tooth disease 1C. Neurology. 2003;60:22-26.

ACKNOWLEDGEMENTS

We thank Drs. M.D.Odero (Pamplona, Spain), Frances Sole (Barcelona, Spain) and J.C.Cigudosa (Madrid, Spain) for assistance with color cytogenetic analyses; and Drs. A.Turhan (Paris, France) and A. Karpas (Cambridge, UK) for kindly providing UPN-1 and UPN-2 cell lines, and Karpas 1718 cell line, respectively.

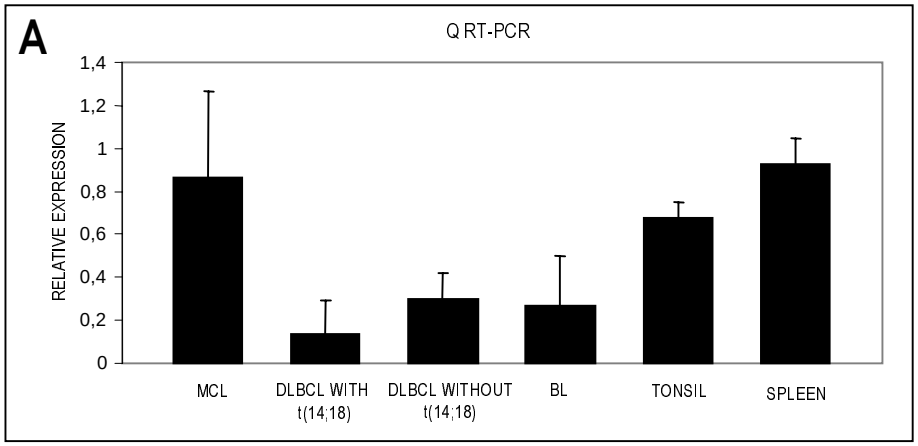
A
Q RT-PCR
RELATIVE EXPRESSION
1,4
1,2
1
0,8
0,6
0,4
0,2
0
MCL
DLBCL WITH t(14;18)
DLBCL WITHOUT t(14;18)
BL
TONSIL
SPLEEN

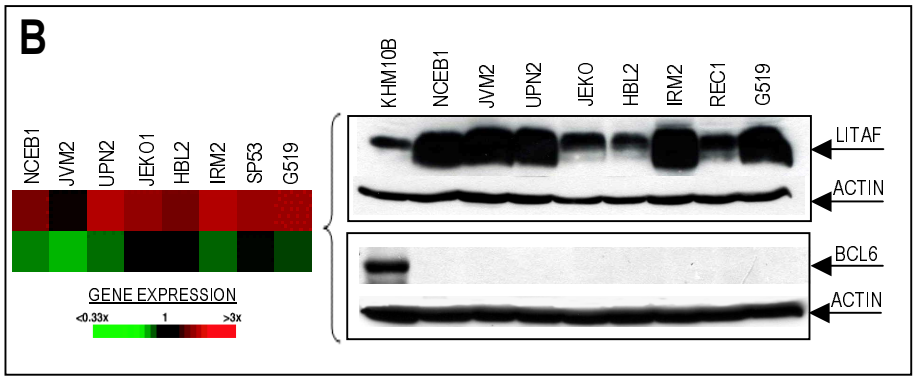
B
NCEB1
JVM2
UPN2
JEKO1
HBL2
IRM2
SP53
G519
GENE EXPRESSION
<0.33x
1
>3x
KHM10B
NCEB1
JVM2
UPN2
JEKO
HBL2
IRM2
REC1
G519
LITAF
ACTIN
BCL6
ACTIN

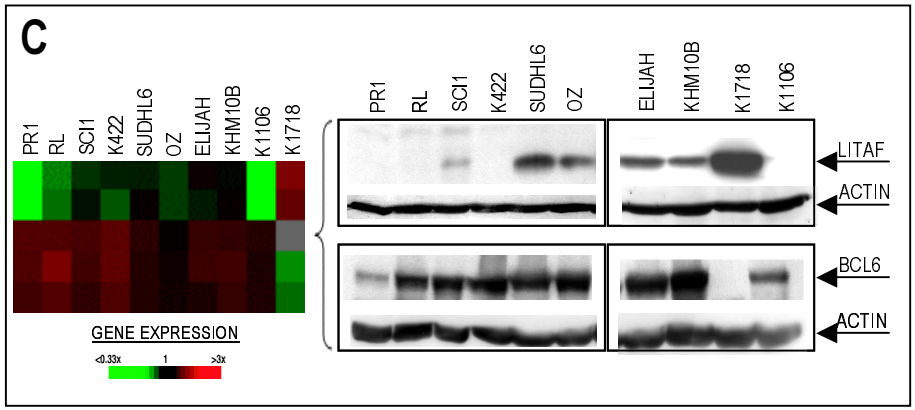
C
PR1
RL
SCI1
K422
SUDHL6
OZ
ELIJAH
KHM10B
K1106
K1718
GENE EXPRESSION
<0.33x
1
>3x
PR1
RL
SCI1
K422
SUDHL6
OZ
ELIJAH
KHM10B
K1718
K1106
LITAF
ACTIN
BCL6
ACTIN

FIGURE 1

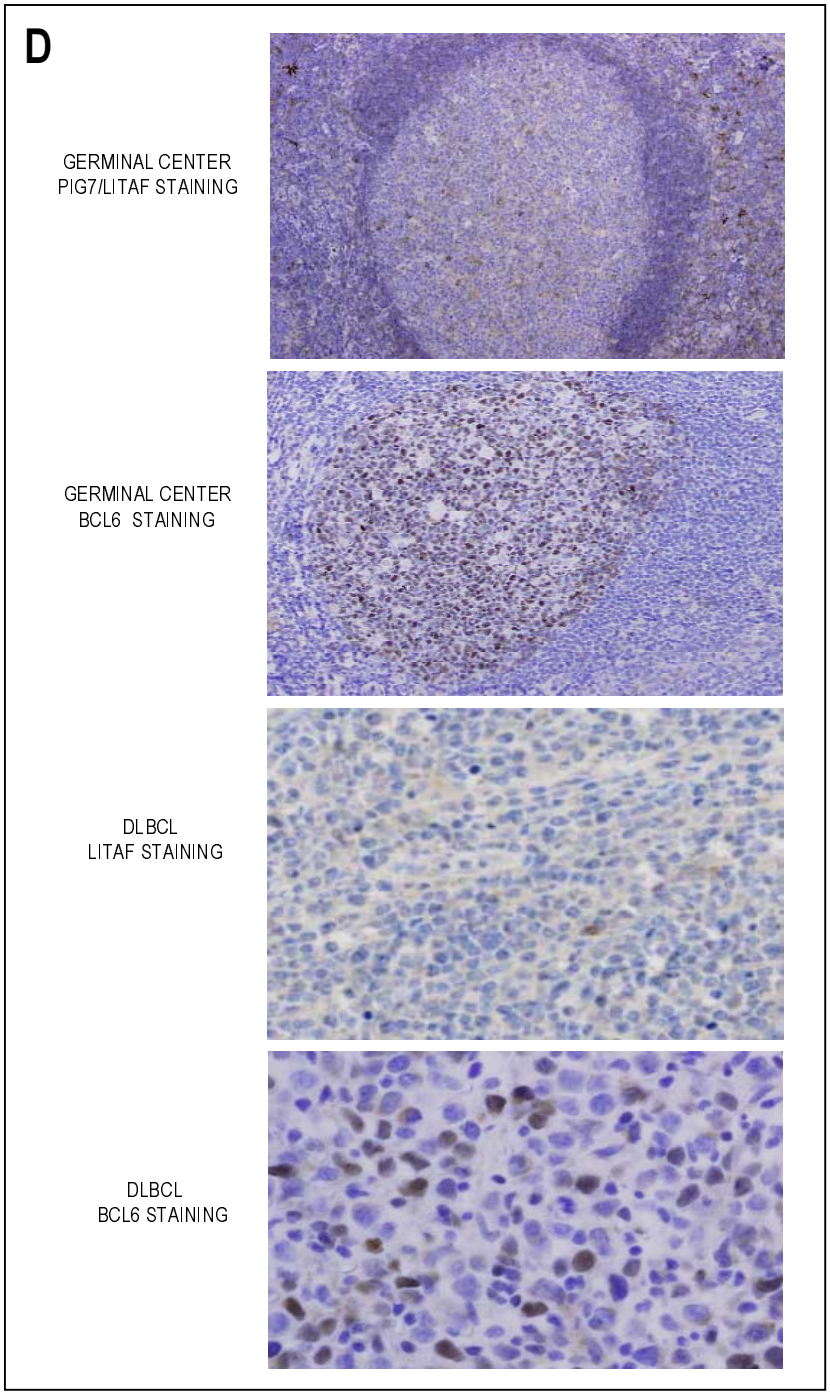
D
GERMINAL CENTER
PIG7/LITAF STAINING
GERMINAL CENTER
BCL6 STAINING
DLBCL
LITAF STAINING
DLBCL
BCL6 STAINING

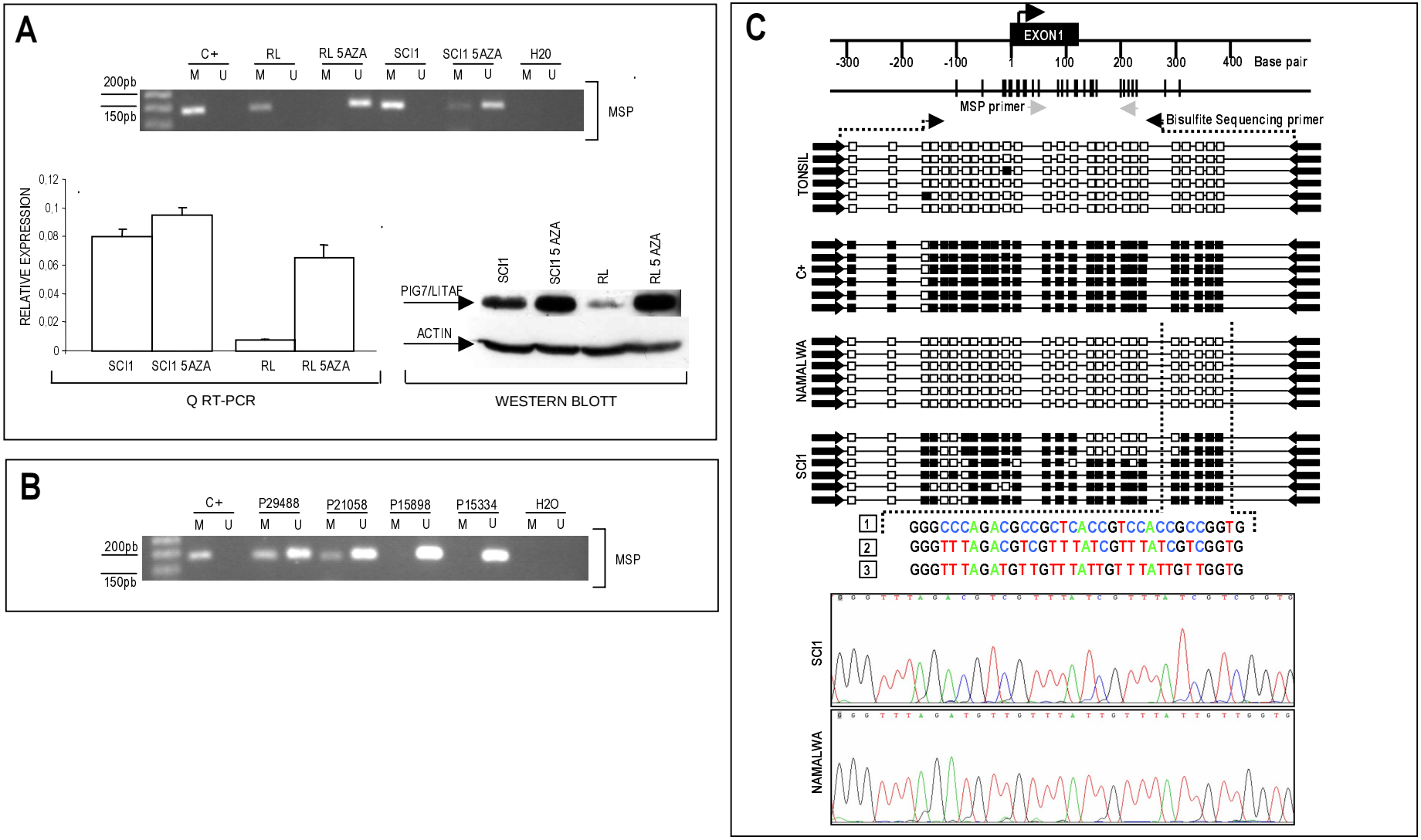
A
C+
RL
RL 5AZA
SCI1
SCI1 5AZA
H20
M U
200pb
150pb
MSP
RELATIVE EXPRESSION
0,12
0,1
0,08
0,06
0,04
0,02
0
SCI1
SCI1 5AZA
RL
RL 5AZA
Q RT-PCR
PIG7/LITAF
ACTIN
SCI1
SCI1 5 AZA
RL
RL 5 AZA
WESTERN BLOTT
B
C+
P29488
P21058
P15898
P15334
H2O
M U
200pb
150pb
MSP
C
EXON1
-300
-200
-100
1
100
200
300
400
Base pair
MSP primer
Bisulfite Sequencing primer
TONSIL
C+
NAMALWA
SCI1
1 GGGCCCAGACGCCGCTCACCGTCCACCGCCGGTG
2 GGGTT TAGACGTCGT T TATCGTT TATCGTCGGTG
3 GGGTT TAGATGT TGTT TATTGT T TATTGT TGGTG
SCI1
NAMALWA

FIGURE 2

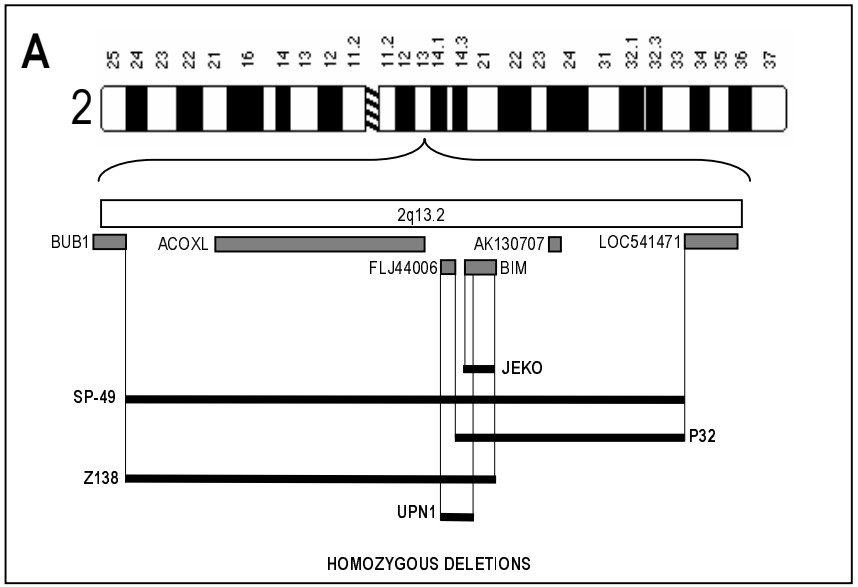
A
2
2q13.2
BUB1
ACOXL
AK130707
LOC541471
FLJ44006
BIM
JEKO
SP-49
P32
Z138
UPN1
HOMOZYGOUS DELETIONS

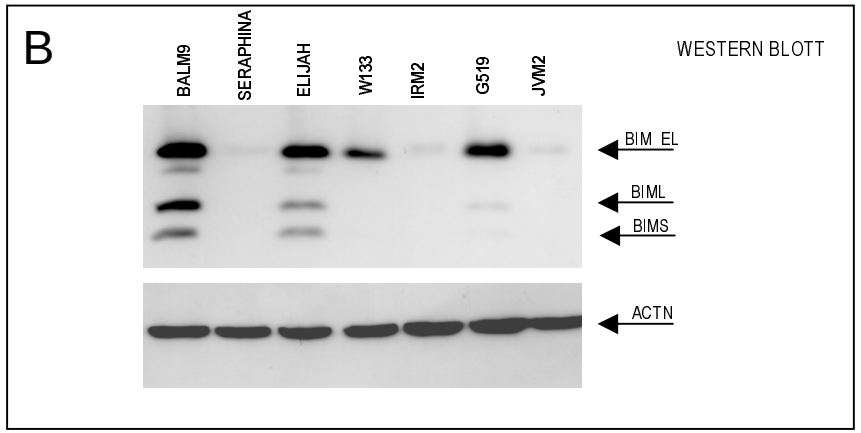
B
WESTERN BLOTT
BALM9
SERAPHINA
ELIJAH
W133
IRM2
G519
JVM2
BIM EL
BIML
BIMS
ACTN

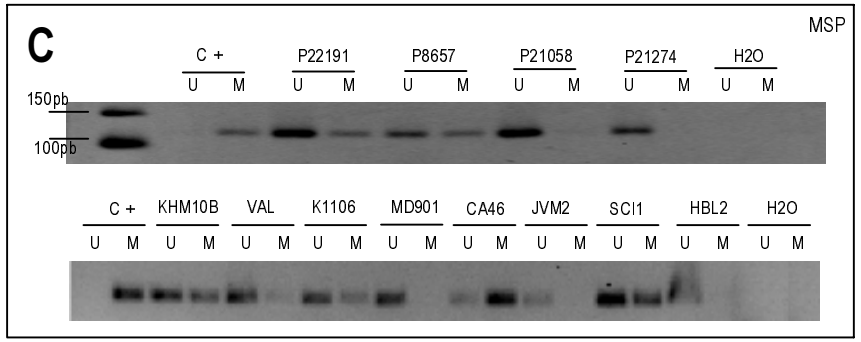
C
MSP
C +
P22191
P8657
P21058
P21274
H2O
U M
150pb
100pb
KHM10B
VAL
K1106
MD901
CA46
JVM2
SCI1
HBL2

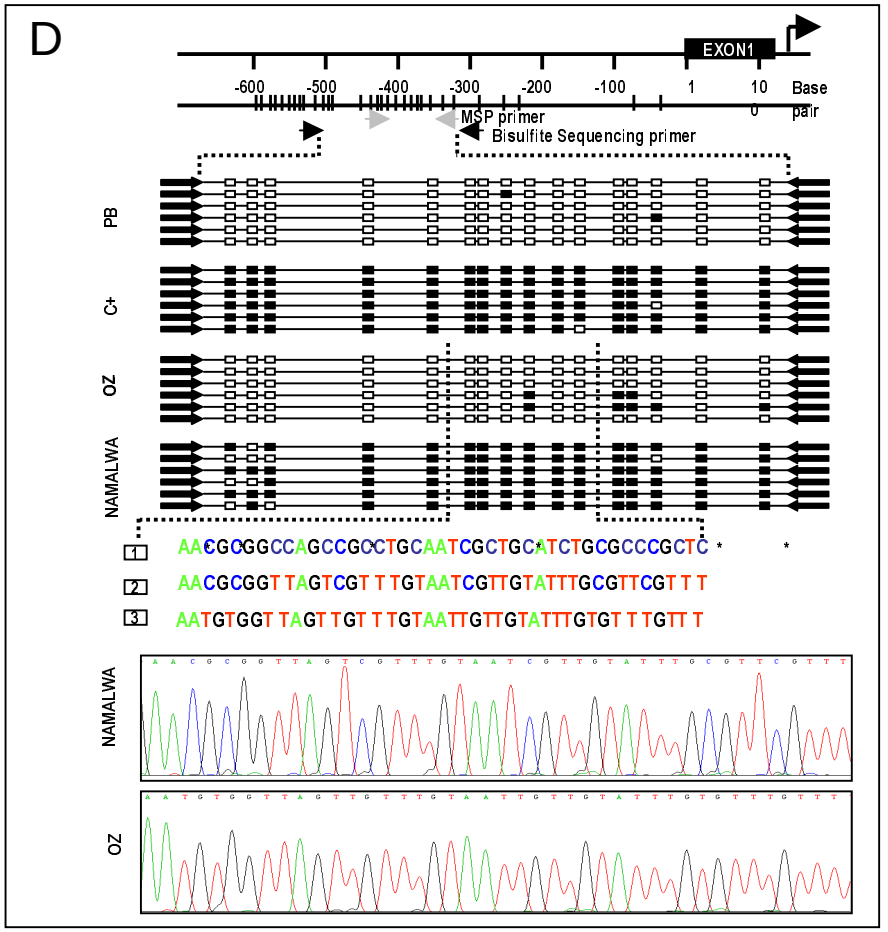
D
EXON1
-600
-500
-400
-300
-200
-100
1
10
Base pair
MSP primer
Bisulfite Sequencing primer
PB
C+
OZ
NAMALWA
AACGCGGGCCAGCCGCCTGCAATCGCTGCATCTGCGCCCGCTC
AACGCGGTTAGTCGTTTGTAATCGTTGTATTTGCGTTCGTTT
AATGTGGTTAGTTGTTTGTAATTGTTGTATTTGTGTTTGTTT

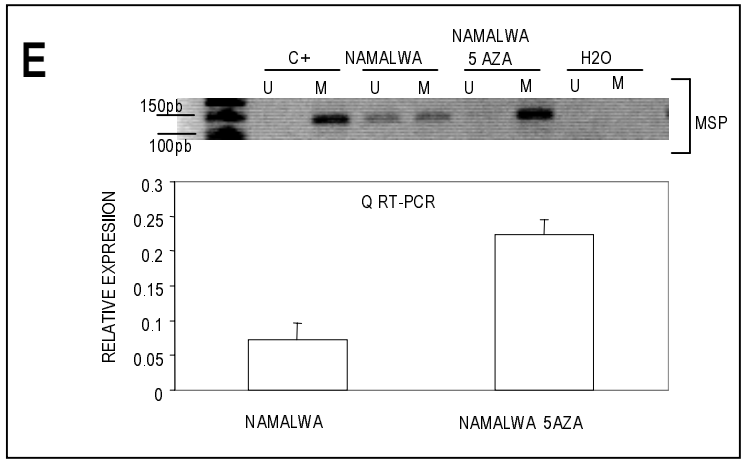
E
NAMALWA
C+
NAMALWA
5 AZA
H2O
U M
150pb
100pb
MSP
Q RT-PCR
RELATIVE EXPRESSION
0.3
0.25
0.2
0.15
0.1
0.05
0
NAMALWA
NAMALWA 5AZA

FIGURE 3

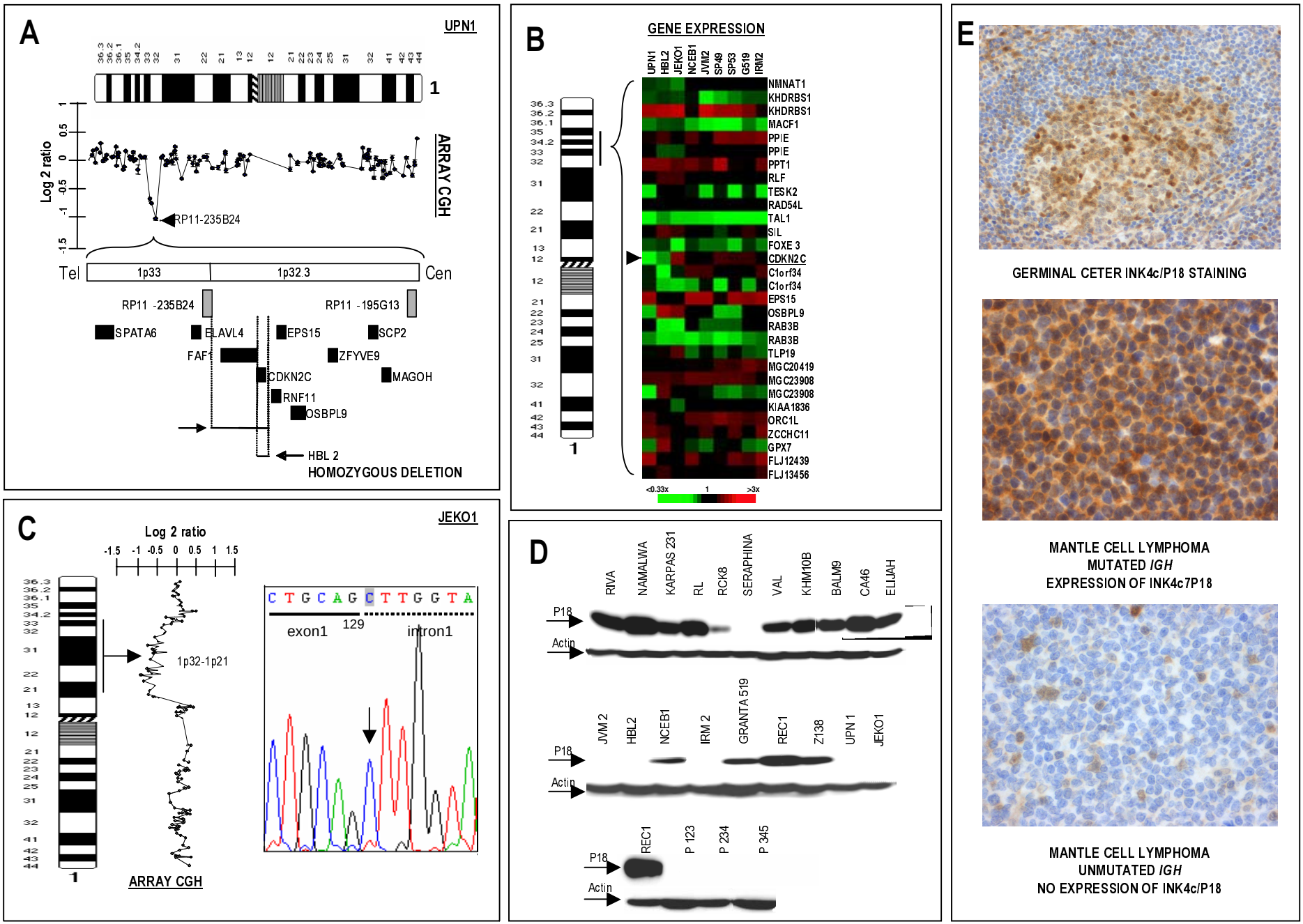
A
UPN1
Log 2 ratio
ARRAY CGH
RP11-235B24
Tel
1p33
1p32.3
Cen
RP11 -235B24
RP11 -195G13
SPATA6
ELAVL4
EPS15
SCP2
FAF1
ZFYVE9
CDKN2C
MAGOH
RNF11
OSBPL9
HBL 2
HOMOZYGOUS DELETION
B
GENE EXPRESSION
UPN1
HBL2
JEKO1
NCEB1
JVM2
SP49
SP53
G519
IRM2
NMNAT1
KHDRBS1
KHDRBS1
MACF1
PPIE
PPIE
PPT1
RLF
TESK2
RAD54L
TAL1
SIL
FOXE 3
CDKN2C
C1orf34
C1orf34
EPS15
OSBPL9
RAB3B
RAB3B
TLP19
MGC20419
MGC23908
MGC23908
KIAA1836
ORC1L
ZCCHC11
GPX7
FLJ12439
FLJ13456
<0.33x
1
>3x
C
JEKO1
Log 2 ratio
1p32-1p21
ARRAY CGH
C T G C A G C T T G G T A
exon1
129
intron1
D
RIVA
NAMALWA
KARPAS 231
RL
RCK8
SERAPHINA
VAL
KHM10B
BALM9
CA46
ELIJAH
P18
Actin
JVM 2
HBL2
NCEB1
IRM 2
GRANTA 519
REC1
Z138
UPN 1
JEKO1
P18
Actin
REC1
P 123
P 234
P 345
P18
Actin
E
GERMINAL CETER INK4c/P18 STAINING
MANTLE CELL LYMPHOMA
MUTATED IGH
EXPRESSION OF INK4c7P18
MANTLE CELL LYMPHOMA
UNMUTATED IGH
NO EXPRESSION OF INK4c/P18

FIGURE 4

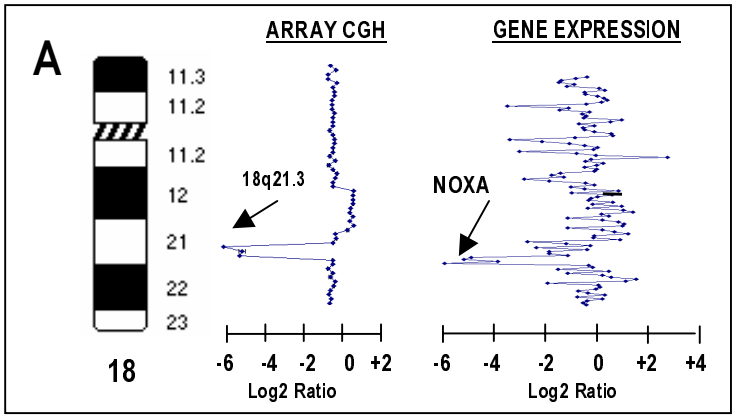
A
ARRAY CGH
GENE EXPRESSION
11.3
11.2
11.2
12
21
22
23
18
18q21.3
NOXA
-6 -4 -2 0 +2
Log2 Ratio
-6 -4 -2 0 +2 +4
Log2 Ratio


B
K1718
ELIJAH
K1106
G519
NCEB1
P11527
P11844
P11691
TONSIL
NOXA
10kD
ACTIN
37kD

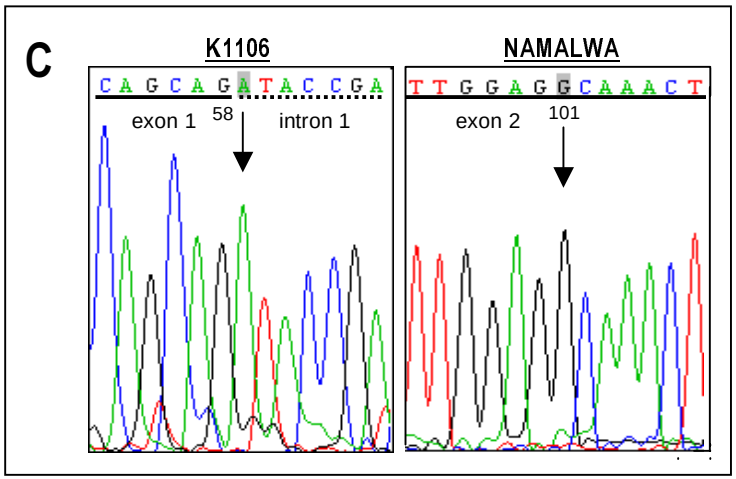
C
K1106
NAMALWA
C A G C A G A T A C C G A
T T G G A G G C A A A C T
exon 1
58
intron 1
exon 2
101

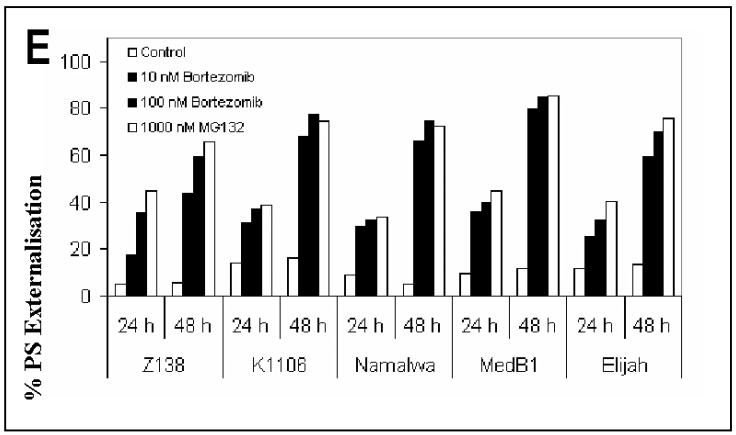
E
Control
10 nM Bortezomib
100 nM Bortezomib
1000 nM MG132
% PS Externalisation
100
80
60
40
20
0
24 h
48 h
Z138
K1106
Namalwa
MedB1
Elijah

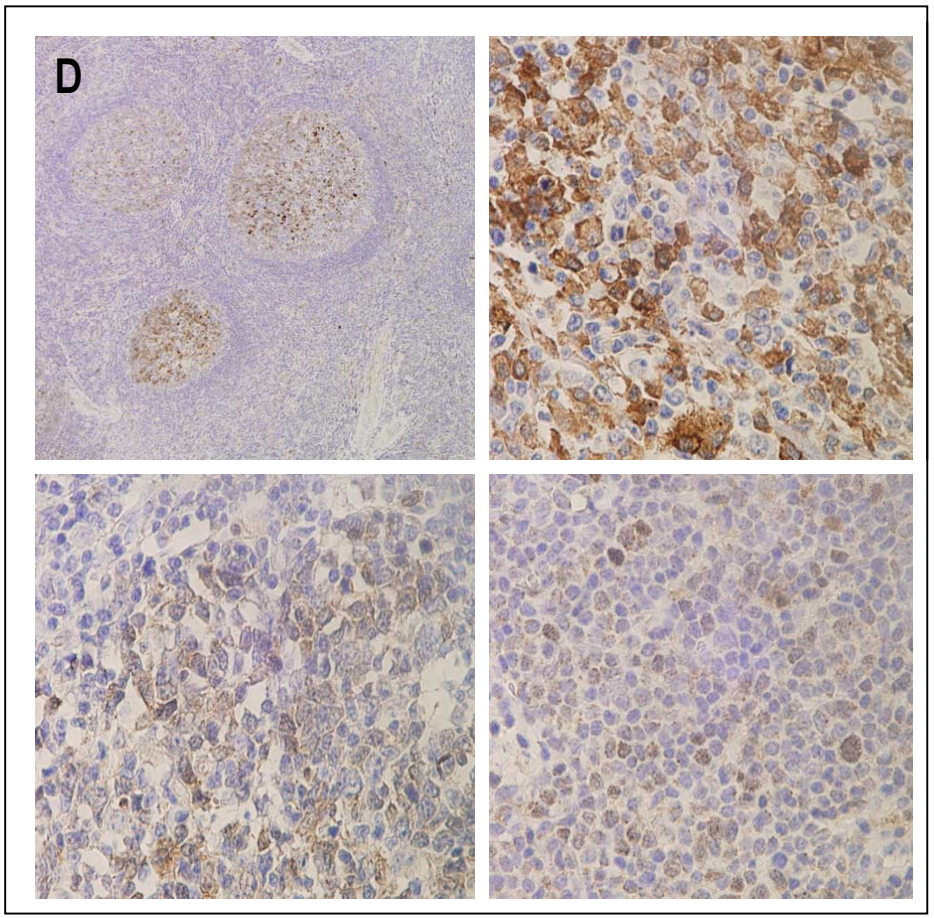
D

FIGURE 5

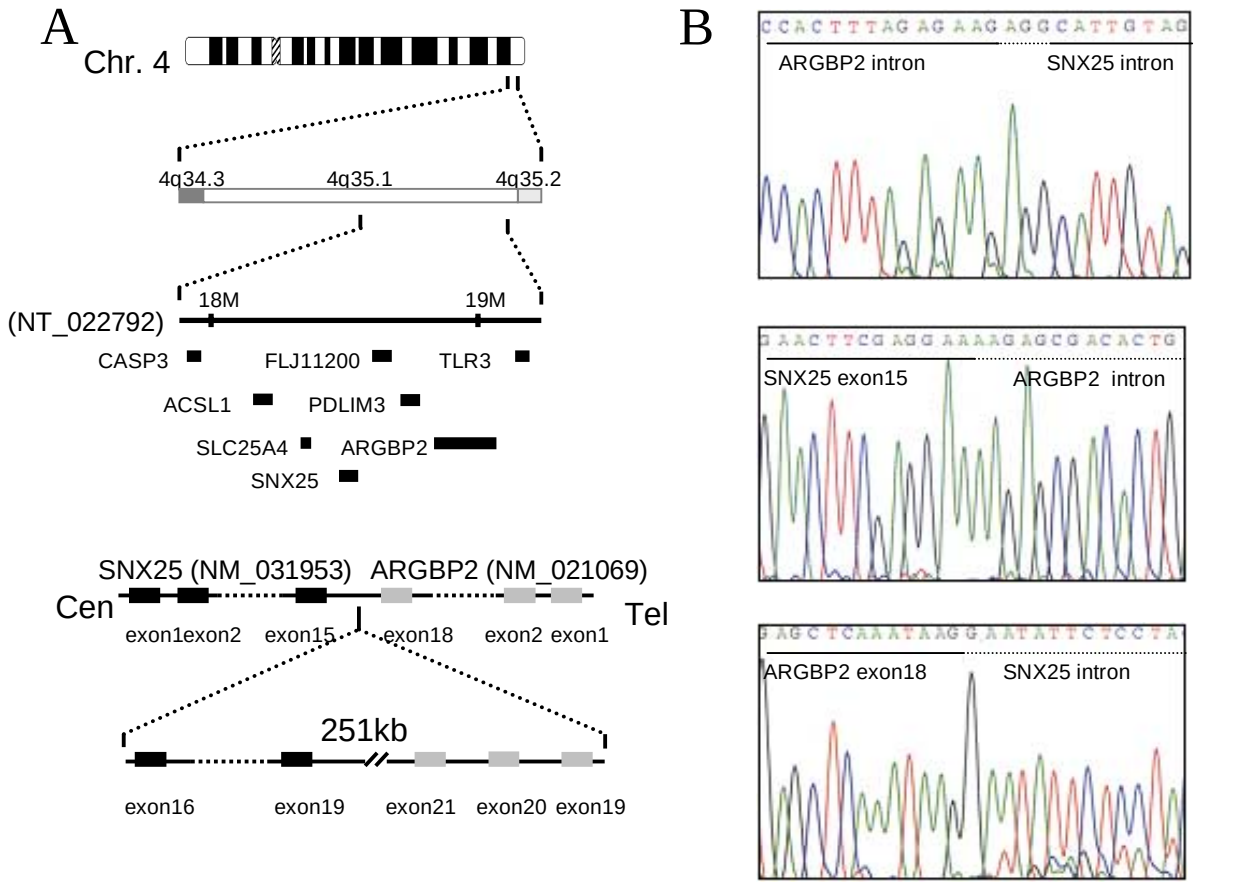
A
Chr. 4
4q34.3
4q35.1
4q35.2
18M
19M
(NT_022792)
CASP3
FLJ11200
TLR3
ACSL1
PDLIM3
SLC25A4
ARGBP2
SNX25
SNX25 (NM_031953)
ARGBP2 (NM_021069)
Cen
Tel
exon1exon2
exon15
exon18
exon2 exon1
251kb
exon16
exon19
exon21
exon20 exon19
B
ARGBP2 intron
SNX25 intron
SNX25 exon15
ARGBP2 intron
ARGBP2 exon18
SNX25 intron
C
Truncated SNX25
exon1exon2
exon15
ARGBP2 intron
Truncated ARGBP2
exon1exon2
exon18
SNX25 intron
D
Elijah
HRC57
MD901
SUPB15
SNX25 exon12-15
SNX25 exon16-19
GAPDH

FIGURE 6